5-2015

Design, Testing, and Calibration of a Custom Air Data Boom to Obtain Flight Data For the UTSI Cessna-T210J (N33UT)

Kristopher Nathaniel Oegema
University of Tennessee - Knoxville, koegema@utsi.edu

To the Graduate Council:

I am submitting herewith a thesis written by Kristopher Nathaniel Oegema entitled "Design, Testing, and Calibration of a Custom Air Data Boom to Obtain Flight Data For the UTSI Cessna-T210J (N33UT)." I have examined the final electronic copy of this thesis for form and content and recommend that it be accepted in partial fulfillment of the requirements for the degree of Master of Science, with a major in Engineering Science.

Steve Brooks, Major Professor

We have read this thesis and recommend its acceptance:

Peter Solies, Borja Martos

Accepted for the Council:
Carolyn R. Hodges

Vice Provost and Dean of the Graduate School

(Original signatures are on file with official student records.)

Design, Testing, and Calibration of a Custom Air Data Boom to Obtain Flight Data For the UTSI Cessna-T210J (N33UT)

A Thesis Presented for the

Masters of Science

Degree

The University of Tennessee, Knoxville

Kristopher Nathaniel Oegema

May 2015

DEDICATION

This thesis is dedicated to my father Gerald Richard Oegema, for preparing me to face all the challenges that await me.

ACKNOWLEDGEMENTS

I am immensely grateful to the members of my committee, Dr. Steve Brooks, Dr. Borja Martos, and Dr. Peter Solies, for all their help and support on this project and throughout my time at UTSI which I have enjoyed immensely. I would like to thank Greg Heathery and Jacob Bowman, for their help in designing, manufacturing the parts for, and installing the boom onto the Cessna 210. I would also like to thank Jonathan Kolwyck, for his help calibrating the boom and using Solid Works. Finally I would like to thank Larrissa Webb, for her help in proof reading and checking my paper.

ABSTRACT

Flight testing is dependent on the ability to accurately calculate the flight characteristics of an aircraft during a test. Any error caused by an instrument will grow into potentially larger errors or unacceptable ranges of uncertainty for any flight test calculations. The aircrafts pitot static system is designed to minimize the error in readings caused by the pressure changes resulting in air flying around the aircrafts structure. However, it still does not meet the level of accuracy desired for quality flight testing data. In order to get the most accurate data possible noncommercial equipment is installed on the aircraft for flight testing. One such piece of flight testing equipment is a boom installed on an aircraft wing. The boom extends forward from the wing at least one chord length ahead of the wing's leading edge. By taking readings far enough ahead of the wing's leading edge the airflow and pressure that the instruments read are not affected by the aircraft. This is ideal for collecting static pressure, dynamic pressure, angle of attack, and angle of side slip.

This thesis details the process of designing, installing, testing, and calibrating a boom for a Cessna-210 that collects data from a pitot/static system and alpha and beta vanes placed on a boom attached to the wing. It starts with a general look at the goals of the project and the aircraft being modified. The second section covers the design process of getting rough measurements, location for installation, and materials to be used. Section three uses these models to calculate the stresses and deflection that occur on the boom structure under the worst flight case scenarios. Finally, section four covers the actual ground testing of the equipment and the calibration of the instruments on the boom.

TABLE OF CONTENTS

LIST OF TABLES

LIST OF FIGURES

ABREVIATIONS AND SYMBOLS

A	cross sectional area
A_r	bearing reference area
ac	aerodynamic center
α	angle of attack
β	angle of sideslip
$\bar{c}$	mean chord length
C_d	coefficient of drag
C_l	coefficient of lift
C_{mo}	coefficient of bending about the aerodynamic center
C_n	coefficient of drag for air flow normal to structure
CG	center of gravity
CP	center of pressure
D	drag force
D_b	diameter of bolt
D_i	inside diameter
D_o	outside diameter
DAS	data acquisition system
E	modulus of elasticity
F_p	force perpendicular to axis
F_r	resultant force
F_s	shear force
F_n	force normal to axis
F_{nh}	force normal and horizontal to plane
I	moment of inertia
j	safety factor
l	length
L	lift force

lbf	pounds force
λ	angle relative to the longitudinal axis of the boom
M	bending moment
M_t	torsional moment
P_t	total pressure
P_s	static pressure
q	shear flow
ϕ	angle relative to the lateral axis of the boom
R	reaction force
R_i	inside radius
R_o	outside radius
RPM	rotations per minute
ρ	density
S	frontal surface area
σ_b	ultimate bolt stress
σ_e	Von Mises Equivalent Stress
σ_{max}	maximum surface stress
σ_{shear}	shear strength of material
σ_{ult}	ultimate tensile strength of material
t	thickness
τ	shear stress
τ_b	shear stress on bolt
u	air flow velocity
v	volume
V	velocity
V_A	max maneuvering airspeed unique to aircraft
V_{NE}	max airspeed never to exceed unique to aircraft
w	width
W	weight

x	position aft of boom datum
x_c	position forward of front connector
x_f	distance from datum to force
y	perpendicular distance to the neutral axis
Z	sectional modulus

CHAPTER 1: INTRODUCTION

1.1 Background:

Flight testing requires accurate ways of calculating the numerous variables that occur in flight. One of the most critical variables is the airspeed. Commercial systems installed in aircraft use pitot and static ports located on the aircrafts structure to sample static and ram air and use the differences to calculate airspeed, altitude, and climb or decent rates. These values are useful to the pilot since the published airspeeds for stall, best climb, and other critical conditions correlate to the readings indicated by these instruments. These values only represent the indicated airspeed, however, not the true airspeed. As the air flows around the aircraft structure the pressure and velocity of the air is affected. This means that the air the commercial pitot/static ports sample are not true static or dynamic pressure. The aircraft designers try to place the ports to minimize the error but they only need the system to show readings that are accurate to the published critical airspeed and an error will always occur. For the sake of flight testing, a more accurate reading that represents the physics and true condition of the aircraft are necessary.

To achieve more accurate measurements flight test engineers have several options. These including trailing cones or booms extending ahead of the aircraft from the wing or nose tip. For a smaller aircraft the boom is usually a simpler solution. The boom extends far enough ahead of the aircraft that the pressure and velocity of the air mass it samples has not been affected by the aircraft structure. As a general rule you want a wing tip boom to be at least one chord length ahead of the wing's leading edge or a nose mounted boom to be at least half the fuselage length ahead of the nose. This is a rough estimate for the distance needed for the air to be free from disturbance caused by the aircraft. The dynamic pressure of ram air is sampled from the tip of the boom facing directly into the relative wind,

and the static pressure from a port on the side of the boom facing perpendicular to the relative wind. The ports are connected to transducers in the wing that relate the pressure to digital reading of airspeed and pressure altitude that can be recorded by the data acquisition system onboard the plane.

Since the boom structure minimizes the issues caused by the airflow around the air mass it is also an ideal location for the placement of alpha and beta vanes. These vanes are simple flat plate structures so that the weathercock stability factor causes them turn into the relative wind caused by the aircrafts movement through the air mass. They are positioned in line with the axis of the aircraft to provide the angle of attack, α, or the angle of side slip, β. The angle the vanes deflect from their centered position is measured by a potentiometer that relates the reading to an angle through a calibration. The vanes must be calibrated for individual aircraft since the boom might not be naturally aligned with the zero angle of attack or side slip.

1.2 Aircraft:

This thesis details the design and construction of a boom for a Cessna-210, tail number N33UT, owned by University of Tennessee Space Institute that provides pitot/static, angle of attack, and angle of sideslip data for future flight test purposes at the university. The aircraft is a Cessna-T210L Turbo Centurion model with a Continental IO-520-J engine, fixed gear, a three blade propeller, and modified seating for four [1]. It has been modified to have a data acquisition system, DAS, in the rear of the plane installed in a rack with a power control system that take the place of the two rear seats. The aircraft has also been equipped with an instrument video system, upward and downward facing Radiometer sensors, pyrometer assembly, laser altimeter, and expansion wiring for the DAS. Additionally, a commercial stall kit has been installed on the wings. All this equipment was added for the intent of performing flight test.

1.3 Purpose:

The boom shall be installed on the underside of the right wing tip in a manner that allows it to stay installed while regular maintenance is performed on the aircraft. The boom collects data from the alpha and beta vanes and the pitot/static ports using a Space Age Control Mini Boom [2]. This data provides angle of attack, angle of side slip, altitude, and airspeed information to the flight test engineers. The design must be as light as possible and not produce large amounts of drag so it does not interfere with the aerodynamic qualities of the aircraft, while still structurally strong enough to operate within a safety factor of 1.5 of the materials ultimate strength during all flight conditions that the plane could reasonable experience. If it is found that the boom is a limiting factor for the operations of the aircraft the manual would need to me amended with the new limitations for flight with the boom installed.

The conditions the boom is designed and tested for include a vertical load factor of 4.5 with a horizontal load factor of 1.5. This is above the max G load for a normal category aircraft of 3.8 or utility category of 4.4 [3]. The second condition tested is the aerodynamic drag forces acting on the boom under max airspeed and 20 degree angle of attack and side slip. An angle of 20 degrees was chosen as a conservative value since the max angle of attack for the airfoil before stall is 18-20 degrees and is beyond what could reasonably be performed in a side slip at full speed [4]. These conditions represent beyond the worst case flight operations for the aircraft for the stresses acting on the boom since such dramatic angles of attack and side slip should never be performed above the maneuvering speed for the aircraft. The two worst cases are tested separately, since they add forces in opposite directions and thus one condition would reload the other. The results are used to see if the boom is structurally safe within a minimal factor of 1.5 the ultimate strength. The max deflection of the boom tip is also calculated to ensure the boom does not bend excessively under an applied force. A deflection would shift the boom

and thus the vane mount. While the vanes themselves would still turn into the relative wind, since the mounts shift, the data acquisition system would read a change in angle of attack or side slip depending upon the axis the boom deflects.

Other considerations for the construction of the boom include its effect on the torsional axis of the wing and potential wing bending. The bending moment caused by the boom about the torsional axis of the wing is calculated and compared to the torsional bending moment of the wing at the max maneuvering airspeed to see if the presence of the boom lowers the max airspeed of the aircraft. The natural frequencies of the boom can be reasonably estimated using simulations on a 3D computational model [5]. The results of the model are compared to the frequencies produced by the aircraft at the wing tip to ensure that the design does not oscillate in a manner that would be dangerous to the flight crew.

The boom will only be constructed and installed when a design meets the conditions described above. Once the boom is installed, ground test will be performed prior to any flights. The boom shall be loaded with weights on the ground to simulate a high G load and the calculated aerodynamic loads for the worst case scenarios previously described. The ground test allows the boom to be tested structurally in a safe controlled environment. While still on the ground, the engine shall be slowly powered through the full range of RPM the aircraft might experience in flight to insure that the boom will not achieve natural frequency and begin to oscillate dangerously. When these ground test are performed to satisfaction, the plane can perform a test flight to ensure the boom does not interfere with the maneuvering or safety of the aircraft. Once the testing of the boom has been completed, the booms equipment can be calibrated on the ground and monitored to ensure data flow is consistent and accurate.

CHAPTER 2: DESIGN

2.1 General:

The main consideration for the design of the boom is safety, secondary is good data acquisition and ease of installation and maintenance. The chosen design places the boom on the right wing tip hanging on the underside of the wing attached to a wing spar. This puts the instruments as far from the pressure disturbances of the aircraft as desirable. It was decided to attach the main structure of the boom, orange in Figure 2.1, to the aircraft at three points. Having three connecting points creates an overdetermined system but also provides redundancy in case of a connector failure. This is achieved placing three L brackets, yellow in Figure 2.1, on the inside of the wing attached to the wing spar. Under the wing, widgets, blue in Figure 2.1, are riveted to the L brackets with the wing skin in-between the two. Each widget is a different size associated with the curve of the wing so that the bottom of the widgets should all lie on the same plane in line with the chord line of the wing. Connector, red in Figure 2.1, are machined so that they slip around the main boom structure and connect to the widgets in a double shear connection. The rear connector has a steel aviation bolt that passes though the center of the main structure and the connector that is held in place with a bolt. The three connection system lessens the stress at any single point and adds redundancy for safety.

The main structure of the boom is a series of three tubes fitted together and held rigidly in place with an aviation epoxy. The tubes narrow down from a 1.5” outside diameter to a 1” outside diameter. The tip of the boom has the Space Age Control 100400 Mini Air Data Boom, grey in Figure 2.2, fitted into the smallest tube and held with a drill and tap so that it can be removed and worked on as necessary.

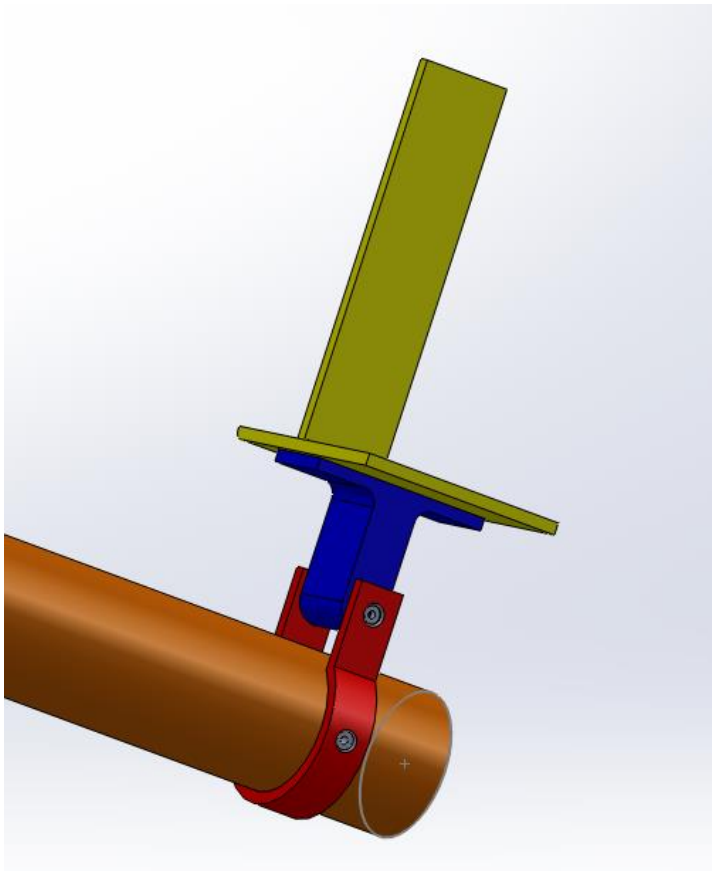

Figure 2.1: Model of Connection Assemble

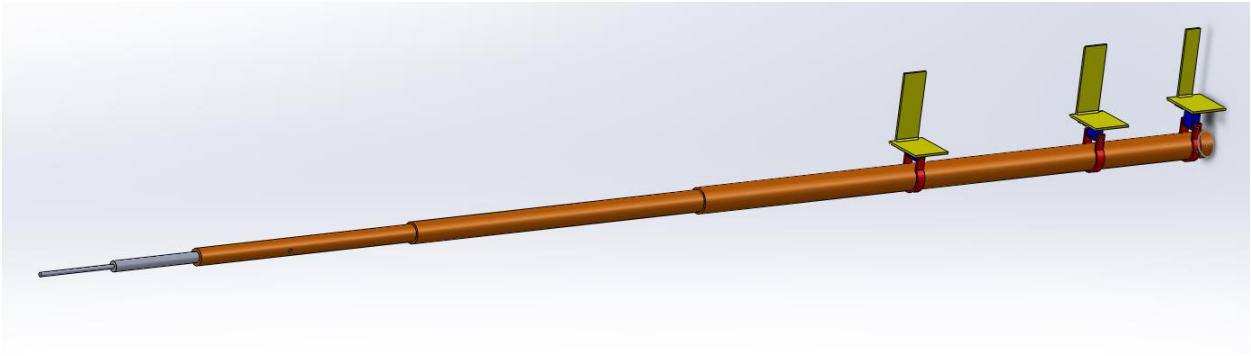

Figure 2.2: Model of Boom

2.2 Main Structure:

The main structure of the boom is made up of three tubes that are machined to be fitted into each other with the minimum clearance from the epoxy specifications. Each progressive tube having an outside diameter that in fits into a bore made in the previous larger tube at a depth of three time the outside diameter of the larger tube. The Space Age Control Boom, Figure 2.3, is attached at the tip of the smallest tube. The exact measurements for the tube structure are shown in Figure 2.4. This makes the main boom structure step down in size as it approaches the tip and have a hollow center to run the instrument's wiring and tubing to the equipment in the wing tip that connects to the DAS. This also means the total wall thickness of the tubes is greater where they overlap. The thicker over laps are not ideal but are a limitation from the machining options present at the time of construction.

At the rear of the boom is a cap that is held in place with the same bolt that connects the rear connector strap to the boom. This end cap is just to cover the opening at the rear of the main structure to prevent foreign objects from getting inside the boom and potentially interfering with instruments or structure. The end cap is fitted tight enough that it does not vibrate in place, but since the end cap does not bear any significant loads on the structure and is held in place by the bolt it does not require as tight a fitting as the tubes. The dimensions of the end cap are shown in Figure 2.5.

The tubing and wiring for the instrument in the Space Age Control Mini Boom are already installed in the tip piece. The length of the tubing or wiring are not very long since the equipment was intended to be a single piece installed on a UAS. The tubing and wiring will have to be extended in order to travel down the boom and reach the equipment in the wing tip.

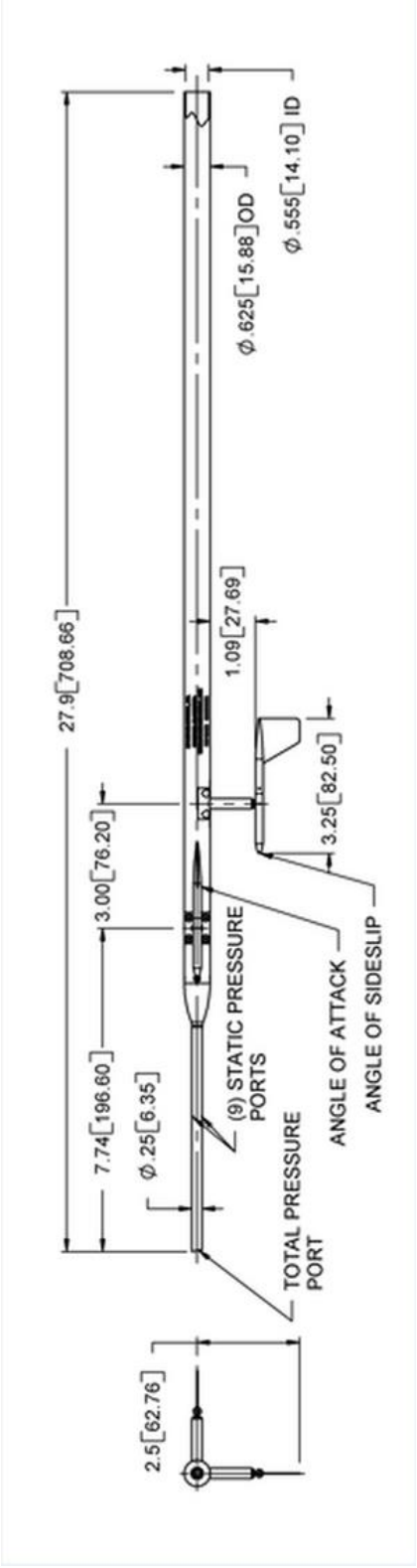

Figure 2.3: Space Age Control Mini Boom 100400 Diagram (from Space Age Controls Inc)

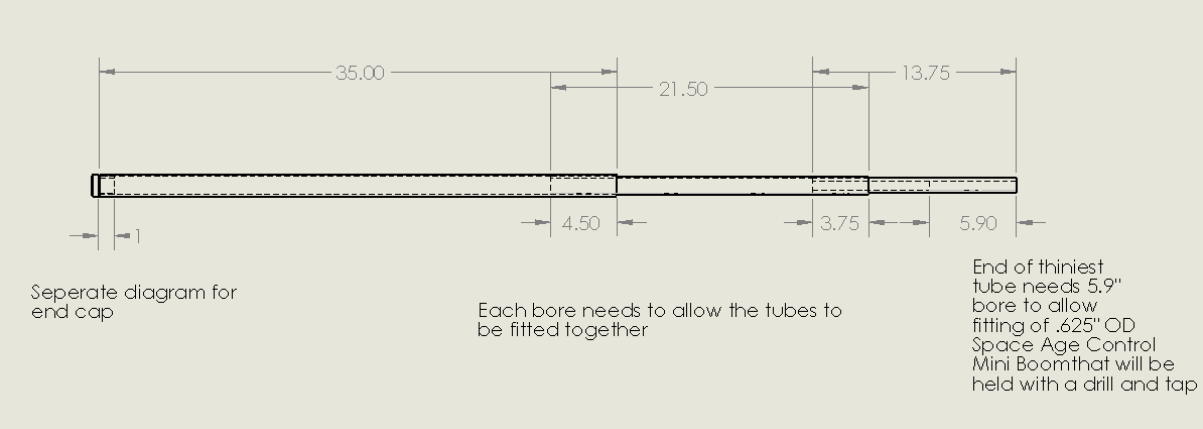

Figure 2.4: Main Tube Structure Drawing

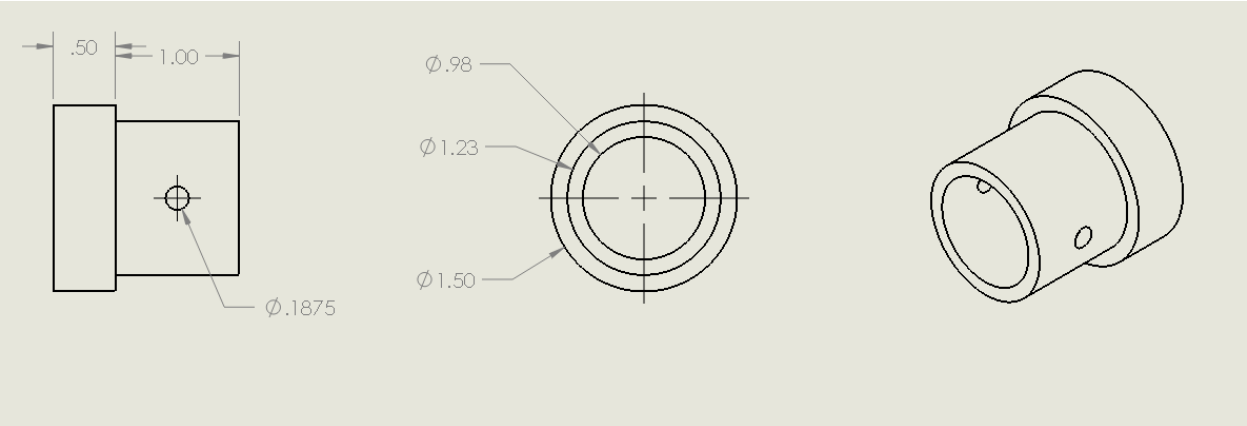

Figure 2.5: End Cap Drawing

2.3 Connectors:

The connectors are machined from AL-6061-T6 to fit around the largest diameter of the main boom structure. They are 1/5” thick and 1/2” wide as the form a semi-circle around the base of the boom so the inside diameter of the connector matches the outside diameter of the boom’s largest pipe. The strap extends upward at the top portion of the semi-circle, 1” above the top of the boom structure and with a gap of 1” between the two sides, show in Figure 2.6.

The 1” inch gap is larger than the widget thickness of .8” so that it creates a pinch around the boom structure when the 3/16 diameter aircraft steel bolt (5Cr-Mo-V) is in place. This pinch holds the boom structure rigidly in place at all three connections. The pinch connection was chosen over having three bolt connections to avoid having to add a bearing stress to the connection that hold the most stress. Not having three bolts also allows the exact location of the connection on the boom to be adjusted slightly while installing the boom to the aircraft. All three connectors are identical in dimensions but the rear connector at the base of the boom has a hole bored for another 3/16 aviation steel bolt to be place through both sides of the connector at the widest portion of the semi-circle, shown in Figure 2.7. This bolt also holds the end cap in place. Due to the impressive strength of aviation steel and the relatively low forces that the boom structure experiences, only one bolt was found to be necessary to bear the forces acting along the boom. The pinch fitting of the connectors is the primary means by which the boom is held ridged. The connectors are machined from blocks of aluminum 6061-t6 with a 32 micron polish finish. A smooth finished is desirable to limit skin drag from airflow around the parts and to avoid structural weak points.

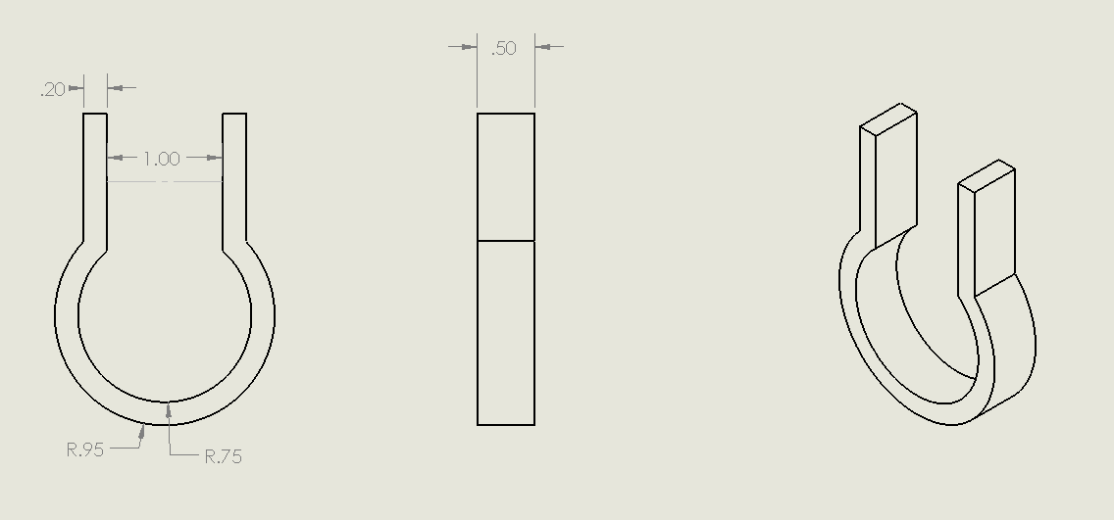

Figure 2.6: Connector Diagram

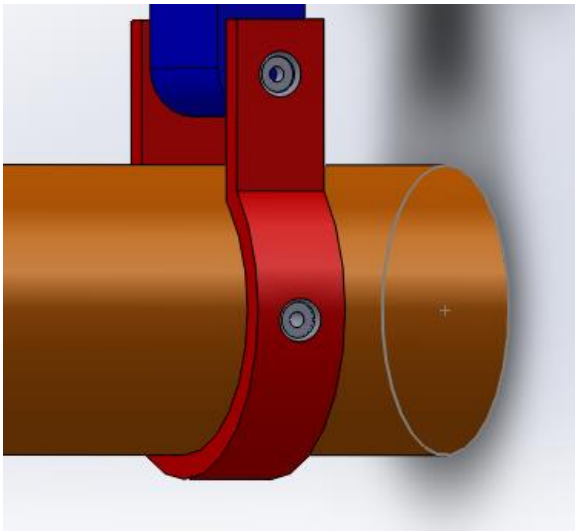

Figure 2.7: Rear Bolt Position

2.4 Widgets:

Each widget has the same basic design, but a unique height fitted to correct for the curve of the wing. The Cessna-T210L has a NACA 2412 airfoil. The airfoil curve data points provided by AirfoilTools.com [4] was adjusted for the chord length and loaded into SolidWorks at a zero angle of attack. The position of lightning holes and the aileron hinge was manually added using measurement off the aircraft. Where the three L bracket could be placed was decided and added to the diagram. A line was plotted to represent the top surface of a boom that would align with the zero angle of attack and clear the stall kit installed on the wing's leading edge, shown in Figure 2.8. The measurements from the L brackets perpendicular to the plotted line where used as the height measurements for the widgets. The measurements were found to be from front to rear .75", 1.15", and 1.25". The measurements were used to create the widget diagrams in Figures 2.8-2.10 shown below. All the widgets are 4/5" wide, 1/2" thick, have rounded ends where a hole is bored to place the aviation bolt, and a flat 2" by .8" base that is 1/8" thick. The widgets are also machined from blocks of aluminum 6061-t6 with a 32 micron polish finish.

The widgets will be attached to the aircraft by rivets that pass through the widget, wing skin, and L bracket. Each widget will have two rivets, one on the leading edge and one on the tailing edge. In theory the widgets should be installed so that all the widget tips lay on a parallel plane to how the boom will be installed. In practice the connectors have extra room to shift where the bolt passes through to adjust to correct for small installation errors.

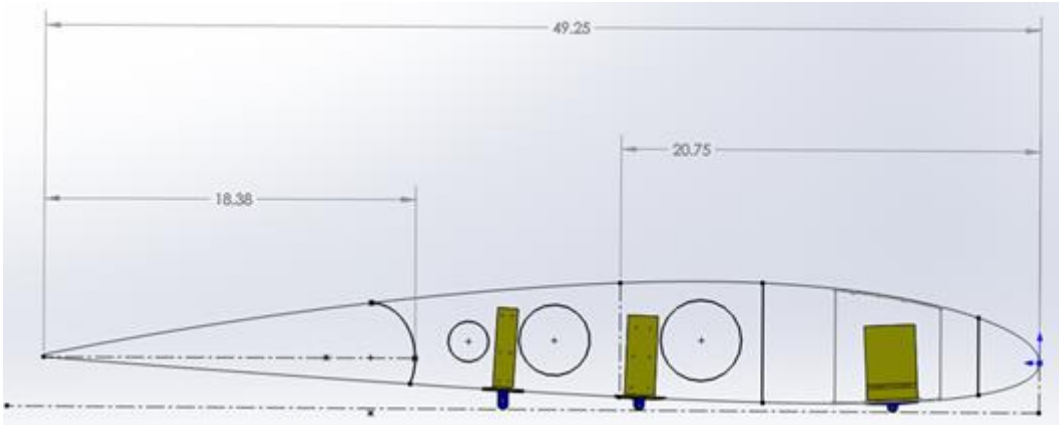

Figure 2.8: Wing layout and positioning of L Brackets

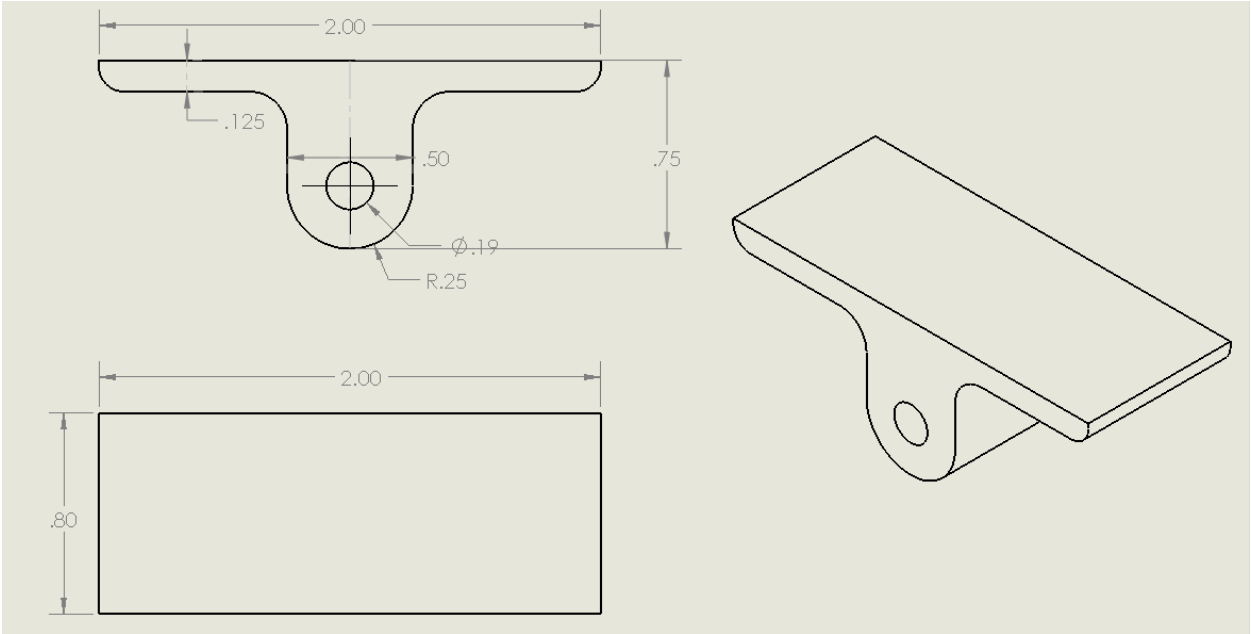

Figure 2.9: Front Widget Diagram

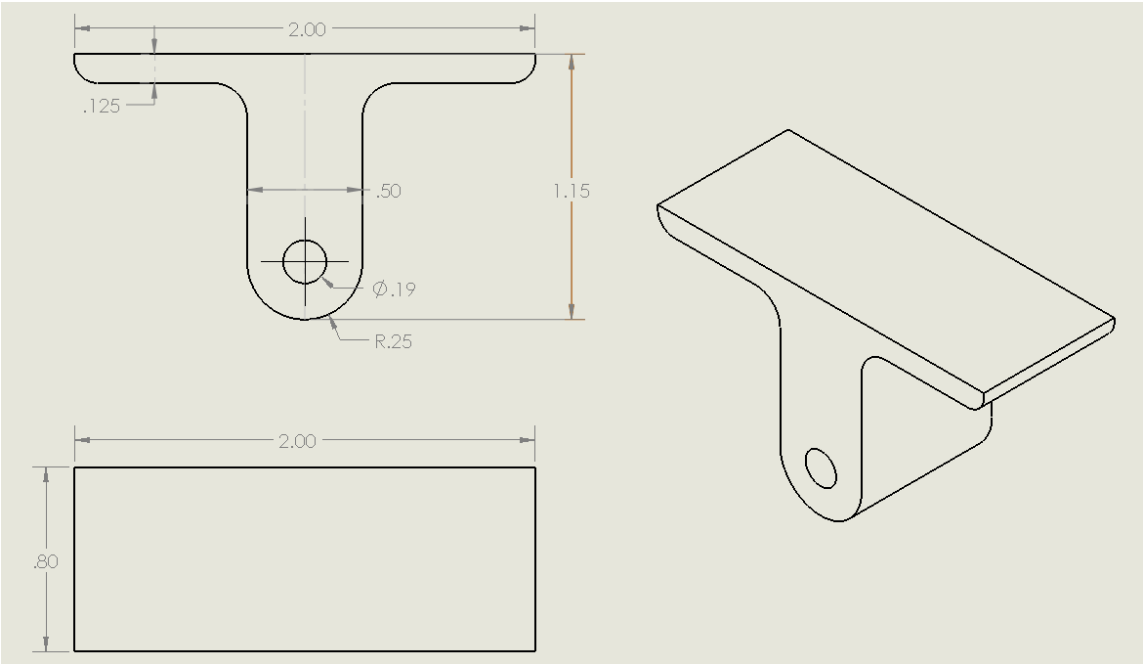

Figure 2.10: Middle Widget Diagram

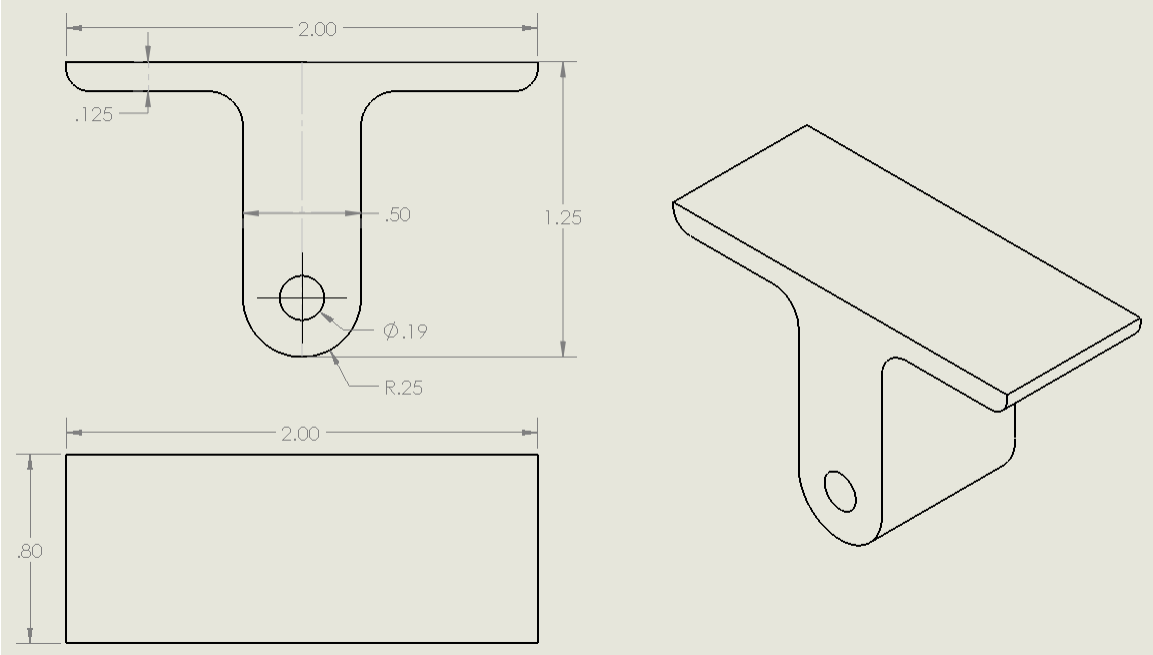

Figure 2.11: Rear Widget Diagram

2.5 L Brackets:

The L brackets are made by bending sheets of aluminum 2024 and each one has unique dimensions to fit between the lightning holes in the win spar. Due to a lack of space on the wing spare for the front bracket, a plate is placed over the lightning hole for the bracket to be connected to. The plate is rived onto the wing spar above and below the lightning hole. Thin plates of aluminum are placed under the L bracket that gradually get smaller as they move from the wing skin to the L bracket, shown in Figure 2.12. The purpose of the plates are to elevate the L bracket .12” over the rivet connecting the spare to the wing skin, and to disperse the force placed on the wing skin gradually.

The center L bracket is a similar design but has to be adjusted due to a wall on the inside of the wing. The wall prevents the bracket from extending to one side so the bracket and step down plates only extend forward and to the side not adjacent to the wall, shown in Figure 2.13. The lack of a step down effect on the side of the wall is not an issue since the added support of the wall will prevent excessive stress from being put on the wing skin. The rear L bracket is the same design with step down plates as the front L bracket. The only difference is the vertical portion is thinner in order to fit between lightning holes on wing spar, shown in Figure 2.14.

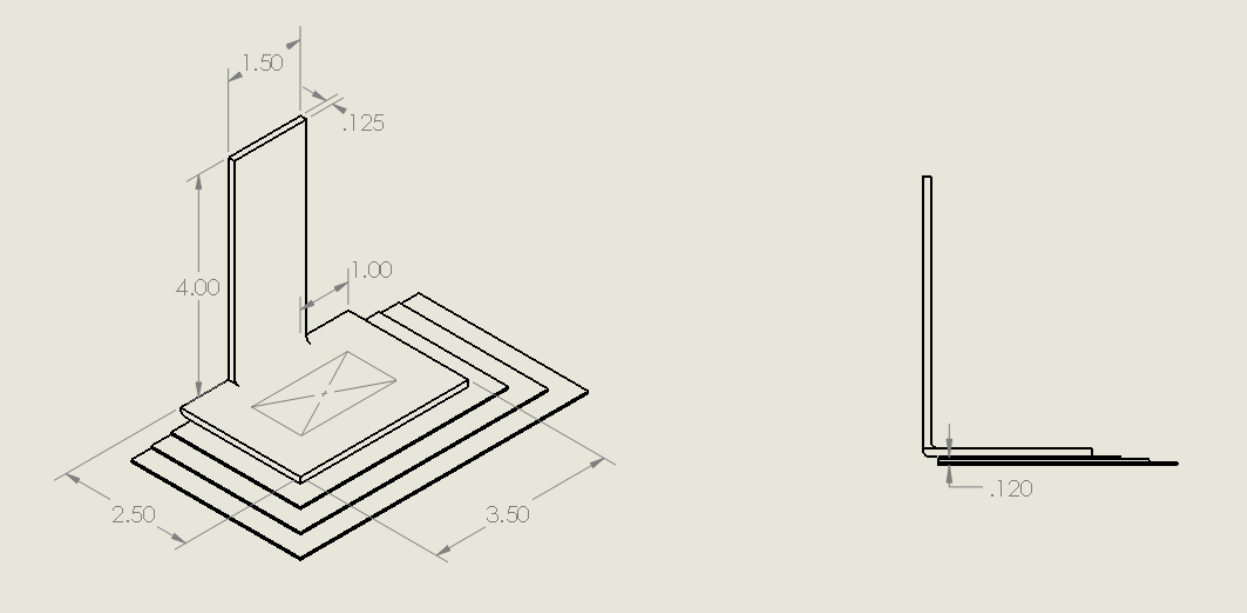

Figure 2.12: Front L Bracket Drawing

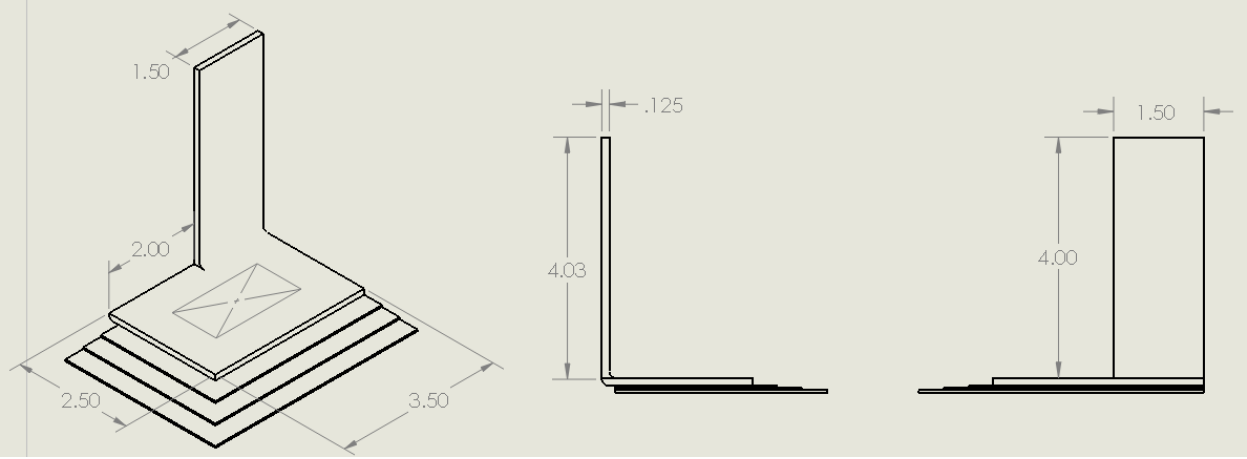

Figure 2.13: Center L Bracket Drawing

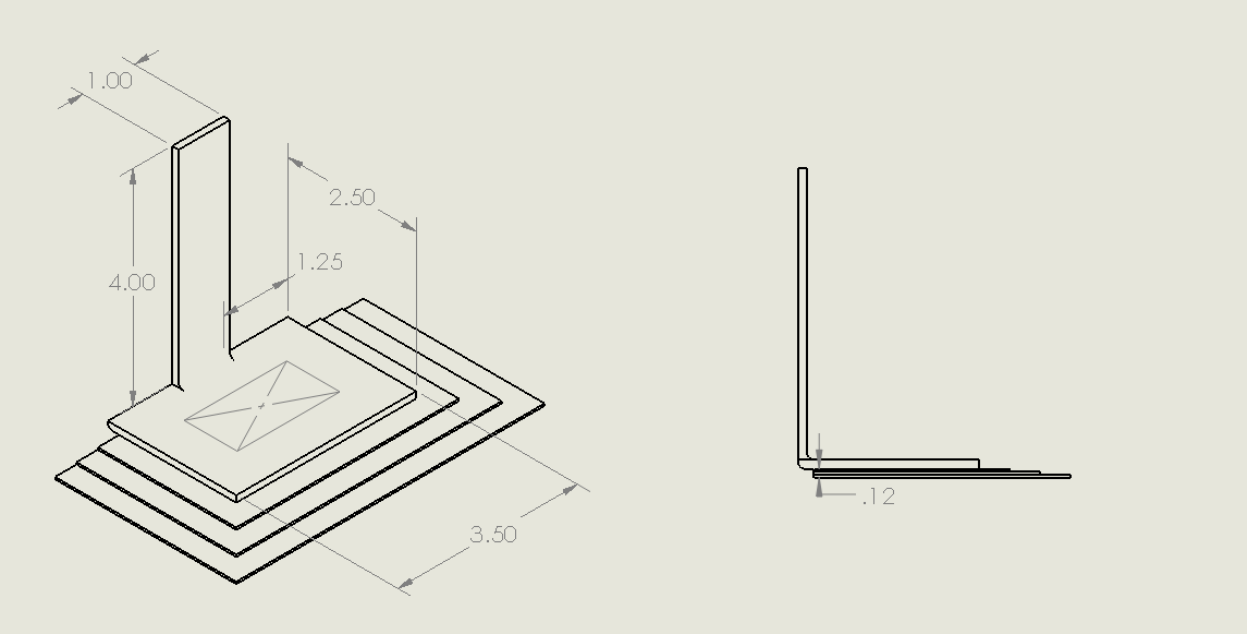

Figure 2.14: Rear L Bracket Drawing

CHAPATER 3: CALCULATIONS

3.1 High G Loading of Boom Structure

To model the worst case G loading situation a force of 4.5 vertical G's and 1.5 horizontal G's is applied to the main structure. This models beyond the highest G loading the aircraft is certified for. The reason for going beyond the rated G loading for the aircraft was to simulate a high G load with additional force from aerodynamic drag or wind gusting. The extra level of safety is good practice since the calculation involves a simplified model and real stresses could differ. To calculate the stresses on the boom, it is divided into sections according to the inside and outside diameter. The sections are named alphabetically starting from the tip of the space age boom and moving aft. Measurements for the sections are shown below in Table 3.1.

Table 3.1: Section Measurements

Section	Length, l (in)	Inside Radius, Ri (in)	Outside Radius, Ro (in)
A	7	0.025	0.125
B	15	0.2775	0.3125
C	5.9	0.2775	0.501
D	4.1	0.31	0.501
E	3.75	0.31	0.6275
F	13.25	0.493	0.6275
G	4.5	0.493	0.7475
H	29.5	0.617	0.7475
I	.5	0	0.75

The weights of each section are found using Equation 3.1.

$$W = \rho * v = \rho * [\left(\frac{\pi 2 R_o^2 l}{4}\right) - \left(\frac{\pi 2 R_i^2 l}{4}\right)] \quad (3.1)$$

The weights for each section are set to act at the center of each section and the moments created by the weight acting at the datum is calculated using Equation 3.2.

$$M = W * x \quad (3.2)$$

A density of .0975 lbs/in^3 for AL 6061-T6 [6] is used to find the weights and moments for sections C through I. Since sections A and B are the pre-purchased mini boom made of a steel-aluminum alloy, the weights provided by Space Age Control [2] for the boom are used to find the weights and moments. All the results are shown in Table 3.2. The total weight of the tube structure is found to be only 4.45 lbs by summing all the sections.

Table 3.2: Section Weights and Moments

Section	Weight, w (lbs)	Location aft of Datum, x (in)	Moment, M (lb-in)
A	0.141	3.500	0.494
B	0.437	14.500	6.333
C	0.452	24.950	11.267
D	0.194	29.950	5.823
E	0.351	33.875	11.885
F	0.611	42.375	25.906
G	0.453	51.250	23.213
H	1.608	68.250	109.760
I	0.172	83.500	14.380

The center of gravity, CG, is found using Equation 3.3 to be 47.305 inches aft of the datum, placing the CG about 14 inches ahead of the wing tip.

$$CG = {\sum M}/{\sum W} = {209.06}/{4.45} = 47.305\ in\ aft\ datum \tag{3.3}$$

The total weight of each section is multiplied by 4.5 and 1.5 to get the critical G load forces. The forces are combined to find the total resultant force of the G loading, Equation 3.5. The resultant forces are divided by the length of their section to get the dispersed load for each section using Equations 3.5. The results of Equation 3.4 and 3.5 are for each section shown in Table 3.3, and the total resultant force acting at the CG is 20.963 lbs.

$$Fr = \sqrt{(4.5 * W)^2 + (1.5 * W)^2} \tag{3.4}$$

$$Fr/in = {Fr}/{l} \tag{3.5}$$

Table 3.3: Resultant Dispersed Loads from G loading

Section	Resultant Force, Fr (lbs)	Dispersed load, Fr/l (lbs/in)
A	0.670	0.096
B	2.072	0.138
C	2.142	0.363
D	0.922	0.225
E	1.664	0.444
F	2.900	0.219
G	2.149	0.477
H	7.628	0.259
I	0.817	0.817

The locations of the reactions are the center of the connectors and are measured on the model at X_{R1}=63.76, X_{R2}=76.30, and X_{R3}=83.00 inches aft of datum. The reaction locations are due to wing geometry and where the L brackets can be connected to the wing rib. The three connections create an over determined system. The over determinate system is solved using an online calculator for over determined systems [7]. The calculator uses the total resultant force acting at the center of gravity of the boom to provides the reaction forces of R_1=57.44 lbs, R_2=53.25 lbs, and R_3=16.78 lbs acting at the connectors. Using the resultant force dispersed loads and the reaction forces it is possible to solve for the shear force, F_s, by summing the forces acting at any point moving aft from the datum, Equation 3.6. The datum for the boom is declared to be the tip of the Space Age Control Mini Boom.

$$F_s = \sum_0^x Fr + \sum_0^x R \tag{3.6}$$

The bending moment at any point aft of the datum is then found as the derivative of the shear forces using Equation 3.7.

$$M = \int_0^x F_s(x)dx \tag{3.7}$$

Figures 3.1 shows the boom divided into sections and Figure 3.2 shows the forces acting on the boom under high G loads using the data from Table 3.3 and Equations 3.6 and 3.7.

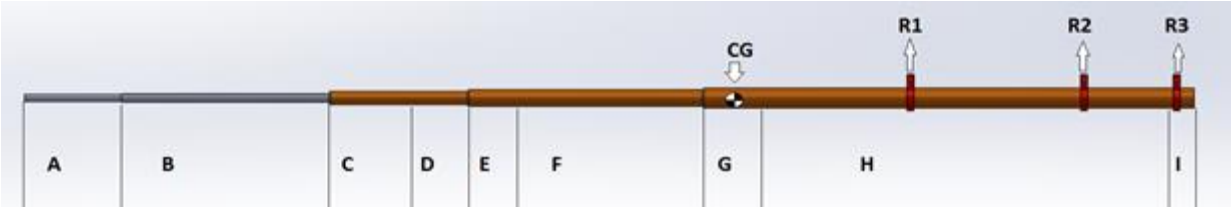

Figure 3.1: Boom Sections

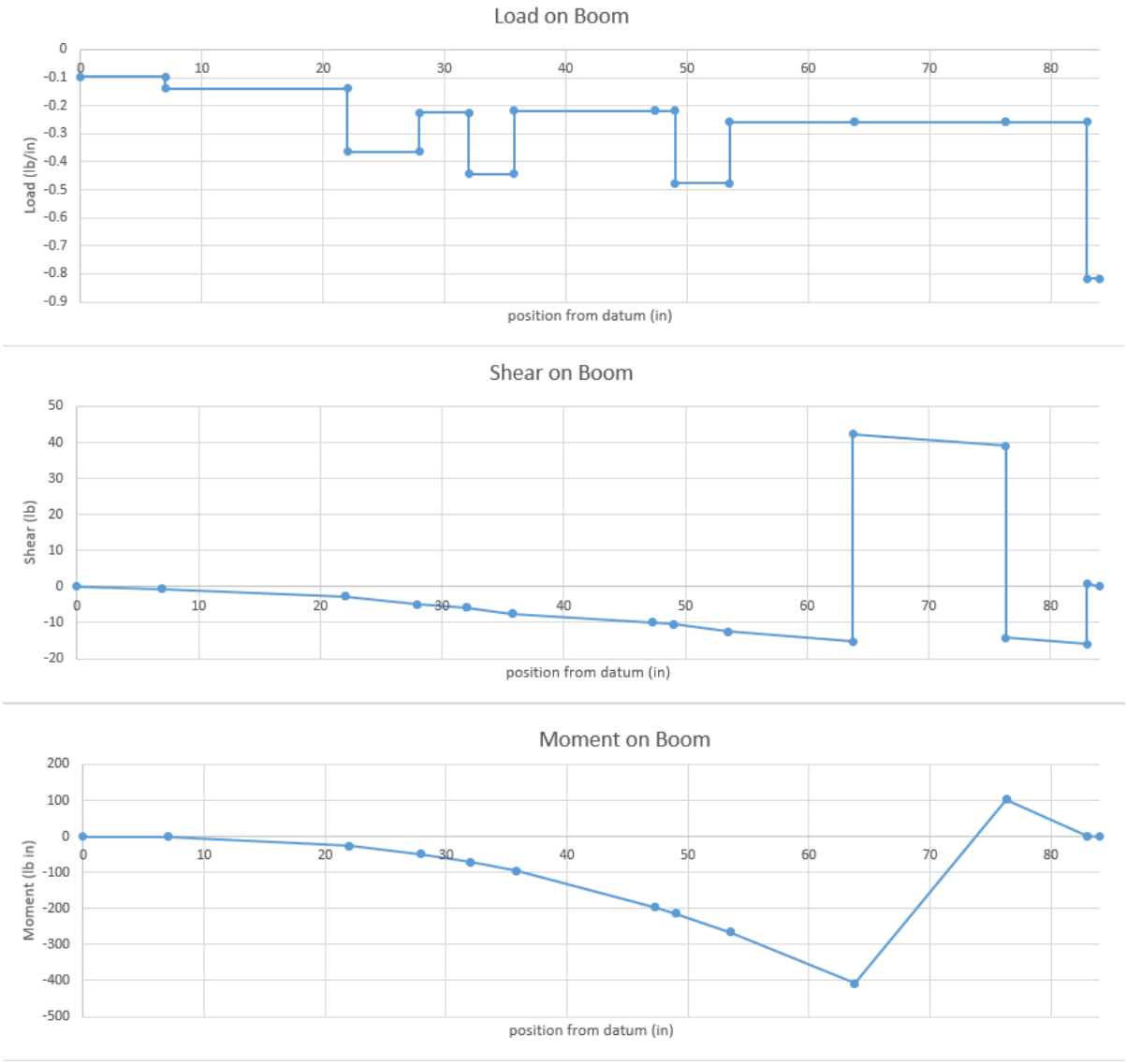

Figure 3.2: Loads, Shear and Bending Moments on Boom under High G Load

The shear forces and cross section area, A, are used to find the shear stress, τ, on a cross section of the boom at any point aft of the datum using Equation 3.8 [8].

$$\tau = {F_s}/{A} = {F_s}/{(\frac{\pi}{4})(D_O^2 - D_i^2)} \tag{3.8}$$

The maximum surface stresses, σ_{max}, caused by the bending moment at any point is calculated using the bending moment, M, and the sectional moduli for a tube, Z, using Equations 3.9 and 3.10. The sectional moduli is a value that represents the flexible qualities of a geometric shapes cross section [9].

$$\sigma_{max} = {M}/{Z} \tag{3.9}$$

$$Z = \frac{\pi(D_O^4 - D_i^4)}{32 * D_o} \tag{3.10}$$

With the surface stress and the shear stress at any point it is possible to find the Von Mises Equivalent Stress, σ_e, using Equation 3.11.

$$\sigma_e = \sqrt{\sigma_{max}^2 + 3\tau^2} \tag{3.11}$$

The Von Mises Stress is commonly used to test designs when a ductile material is used [10]. As long as the Mises Stress is less than the ultimate strength of the material with a safety margin, it is safe to assume the design will not fail. For these calculations it was deemed necessary that all parts of the design would have a minimum safety factor, j, of 1.5 times the ultimate strength of the material to meet the safety requirements of the UTSI flight program. For the purpose of the boom to function as a device that gathers angle of attack and side slip, it is desirable to have a rigid structure that resist deflecting under force, since any deflections in the boom would case an error in the data being recorded. The safety factor is found using an ultimate tensile strength of the material, 45000 psi for ALUM 6061-T6 [6], and Equation 3.12.

$$j = {}^{\sigma_{ult}}/_{\sigma_e} \tag{3.12}$$

Using Equations 3.8 through 3.12 and the data from Figure 3.2 gives the results in Table 3.4 which shows that all the sections of the boom far exceed the strength for safety requirements. This is expected for the boom since it is an aluminum structure that only has to support its own, relatively low, weight since the weight of the vanes, wiring, and tubing is negligible when compared to the main structure. This high safety factor will translate into a relatively unbending structure that will not fluctuate in flight and will provide reliable and accurate data to the flight test crew.

Table 3.4: Stresses in Boom from High G loading

Section	Shear Stress, τ (psi)	Max Surface Stress, σ_{max} (psi)	Von Mises Stress, σ_e (psi)	Safety Factor, j
A	14.20574222	437.0997607	437.791743	102.7885992
B	42.25120726	2895.548942	2896.47357	15.53613345
C	8.933076024	544.7535975	544.973285	82.5728549
D	11.92942408	838.1979434	838.452578	53.67029833
E	7.987841582	523.5092766	523.692066	85.92835936
F	15.77648705	1779.237401	1779.44722	25.28875227
G	12.62109748	997.1783645	997.41795	45.11649304
H	75.55928155	2317.080736	2320.77374	19.39008496
I	0.466136245	2317.080736	2317.08088	19.42141962

A general equation to find estimates for the deflection, y, of the boom under a static load at any location, x, is needed to find the max deflection at the boom tip. Equation 3.13 uses an equation for the moment along with the moment of inertia and the modules of elasticity to find the deflection of the boom at any point aft of the datum [11]. It is derived with respect to the position along the boom twice to get Equation 3.13a. Using the equation generated by Excel from Figure 3.2's moment diagram for the boom portion ahead of the first connector and solving for the constants knowing that dy/dx(0)=0 and y(0)=0 gives Equation 3.13b for the deflection of the boom at a point forward from the first connection, x_c. The modulus of elasticity, E, used for aluminum 6061-T6 is 10,000,000 psi [6]. The area behind the first connector is ignored since the connectors are treated as fixed points in this model and the points behind the first connector will not influence the max deflection of the boom tip.

$$d^2y/dx^2 = M(x_c)/EI_z \tag{3.13}$$

$$y = 1/EI_z \int\int M(x_c)dx_c\,dx_c + C_1x_c + C_2 \tag{3.13a}$$

$$y = (-1.634 * 10^{-8})x_c^4 + (3.624 * 10^{-6})x_c^3 + (-3.000 * 10^{-4})x_c^2 \tag{3.13b}$$

The position is changed from the boom tip moving aft, x, to the first connector moving forward, x_c, for the deflection calculations using Equation 3.14. This is so the total deflection can be summed along the boom starting at the connector and moving towards the tip where the max deflection occurs.

$$x_c = x - 63.76 \tag{3.14}$$

For the value of I, a conservative value of .067 in^4 was chosen to represent the average moment of inertia for the total boom. In reality each section has a different moment of inertia found using Equation 3.15.

$$I = {}^{\pi}/_{4} * (r_o^4 - r_i^4) \quad (3.15)$$

It was attempted to make an equation to represent inertia as a function of position along the boom, $I(x_c)$, that could be derived, however, the values dispersed too greatly for any single equation to fit the data to an acceptable degree. The conservative value of .067 in^4 was chosen by using Equation 3.15 for each section and taking a conservative estimate weighing the size and the moment of inertia for each section. The max deflection at the tip of the boom, $x_c = 63.76$, is conservatively calculated to be .550 inches under a constant static load of 4.5 vertical load factor and 1.5 horizontal load factor. How this relates to an error in the angle experienced by the vane compared to the actual angle of the aircraft is found using Equation 3.16, which uses the length from the first connector to the boom tip and the max deflection to find the angle created. To get the error for the alpha and beta vanes the vertical and horizontal component of the max deflection are used respectively. Knowing that the vertical force is a factor 4.5 and the horizontal is a factor of 1.5, the angel of the max deflection acts at is found to be 18.4 degrees from the vertical plane. Thus the error in the alpha and beta vanes are found using Equations 3.16a and 3.17b

$$error\ in\ angle = \arctan({}^{y_{max}}/_{63.76}) \quad (3.16)$$

$$error\ in\ alpha\ vane = \arctan({}^{y_{max} * \cos(18.4)}/_{63.76}) = .47^o \quad (3.16a)$$

$$error\ in\ beta\ vane = \arctan({}^{y_{max} * \sin(18.4)}/_{63.76}) = .16^o \quad (3.16b)$$

A max induced error in the angle recorded of .47 degrees is an acceptable error for the requirements of the testing the Cessna 210 will be used for. The error will be lost in the general noise of the DAS used onboard the aircraft. The error in the angle being read found in Equation 3.16 is not a position error, but an incurred error caused by having a non-rigid structure being used as a rigid plane of reference. The error is also only .47 degrees under the worst case of G loading, under a standard G load the error will be significantly smaller. This model also assumes that the vanes weight is low enough that the force of G loading on the vane structure is insignificant compared to force of the relative wing acting on the vanes. This is a fair assumption given the CG of the individual vanes should be located close to the pivot and thus G loading does not create a significant turning moment to induce an error.

3.2 Aerodynamic Forces on Boom Structure

S. F. Hoerner's cross flow principle is used to find the drag and lift forces created by the boom at different angles of attack, α, and side slip, β [12]. This principle uses the normal coefficient of drag around a body, C_n, to find the coefficient of drag and lift the body generates at a given angle shown in Figure 3.3. The Principle states that for a cylinder at a given angle:

$$C_d = C_n(sin^3\alpha) \tag{3.17}$$

$$C_l = C_n(sin^2\alpha * \cos\alpha) \tag{3.18}$$

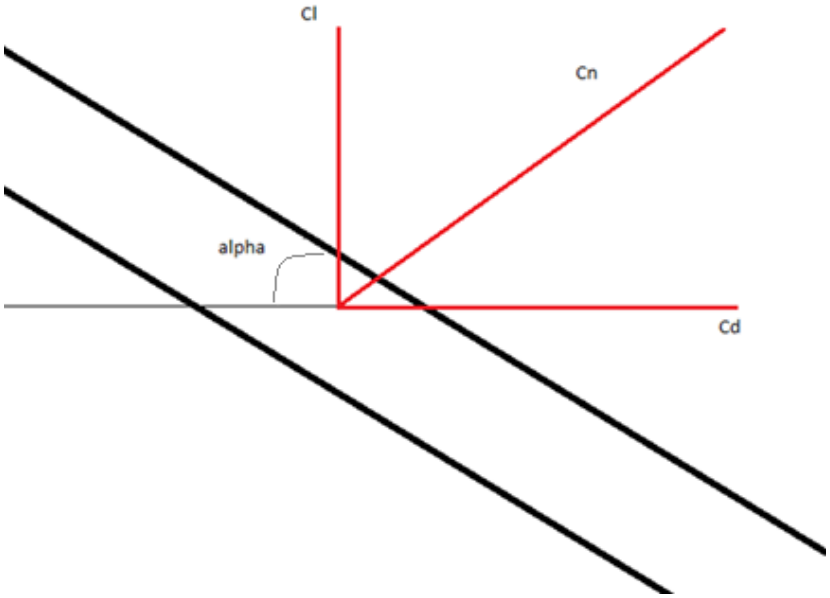

Figure 3.3: Horner's Cross Flow Principle over the Boom

Referring to Hoerner's empirical data for cylinders traveling at the range of Reynolds Numbers, the boom is likely to experience in flight the conservative normal coefficient of drag of C_n=1.17 is found. This gives values of C_l=.1286 and C_d=.0468 for a 20 degrees angle. 20 degrees is the critical condition being calculated since the maximum angle of attack for the aircraft is estimated to be 18-22 degrees. The drag and lift forces are calculated for a density, ρ, of .0023769 slug ft^3 and a velocity, V, of 344.67 ft/s. This is the V_{NE} for the C-210 of 204 knots and the standard sea level air density. In practice the airplane should not have such large angles of attack and side slip above the maneuvering speed of 125 knots. Same as the G loading calculation, the aerodynamic stresses are intentionally over predicted for safety considerations. To model the boom for calculations, the diameter of the largest portion of the boom is used to calculate the value for S. This allows the boom to be treated as a single cylinder and

calculate forces without having to worry about the airflow over where the sections connect. This gives a conservative value for the drag and lift forces acting on the boom since the tip of the boom has a smaller area and will develop less drag and lift.

$$S = D_o * l = .875\ ft^2 \tag{3.19}$$

$$D = C_d \rho * S\ \frac{V^2}{2} = 5.78\ lbf \tag{3.20}$$

$$L = C_l \rho * S\ \frac{V^2}{2} = 15.88\ lbf \tag{3.21}$$

The free body diagram for lift, weight, and drag acting on the simplified boom structure is shown in Figure 3.4.

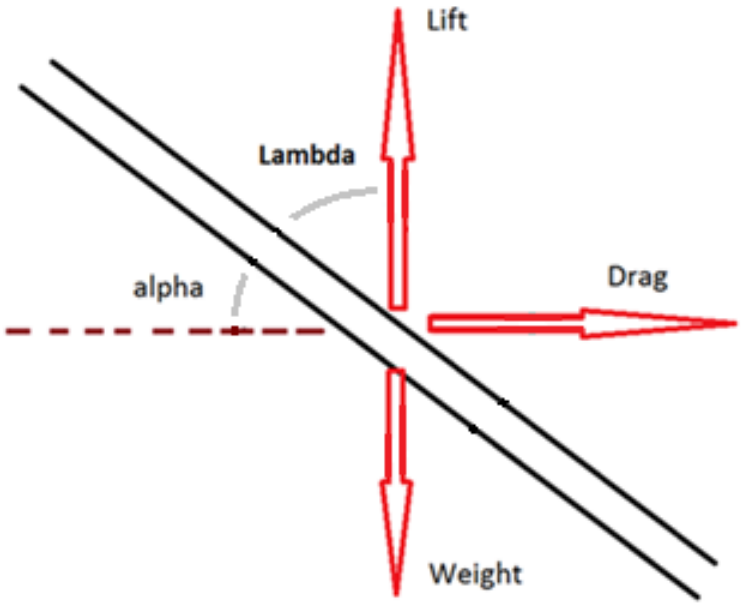

Figure 3.4: Free Body Diagram for Boom at Angle of Attack

The forces found in Equations 3.20 and 3.21 are used to find the forces acting perpendicular and normal to the boom shown in Figure 3.5. The forces perpendicular, F_p, and forces normal, F_n, to the longitudinal plane of the boom are found using Equations 3.22 and 3.23.

$$F_n = (L - W)\sin(\lambda) + D\sin(\alpha) = 16.78\ lbf \tag{3.22}$$

$$F_p = -(L - W)\cos(\lambda) + D\cos(\alpha) = 1.52\ lbf \tag{3.23}$$

This mathematical model shows the boom has 16.78 lbs acting normal to the boom and 1.52 lbs acting perpendicular to the boom for 20 degrees angle of attack. These forces are the sum of dispersed loads acting along the full length of the boom.

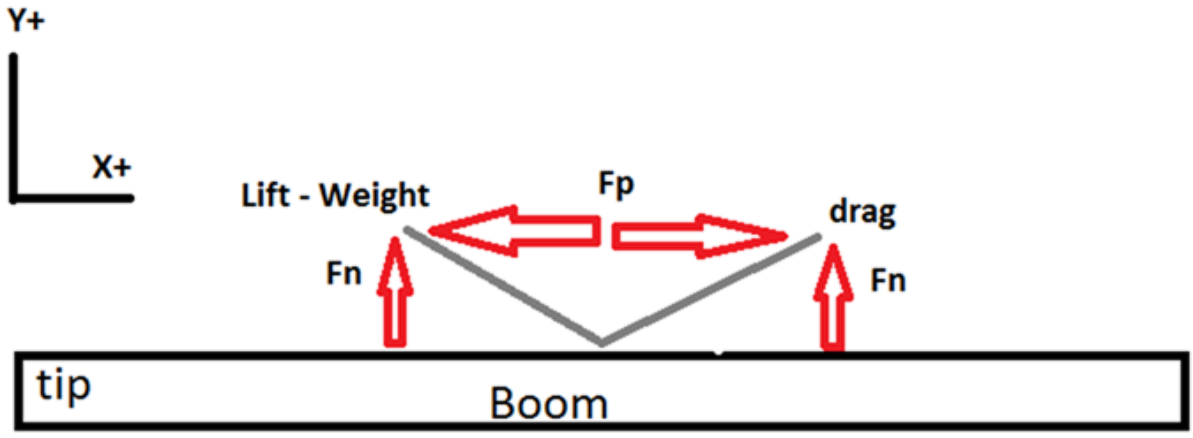

Figure 3.5: Aerodynamic Forces Relative to the Plane of the Boom

The only difference when calculating the horizontal forces caused by the side slip, is that both forces act horizontal to the plane of the boom, and thus weight is no longer acting against one of the vectors, shown in Figure 3.4. The values for drag and lift are still those found using Equations 3.20 and 3.21. The normal and perpendicular forces are then found using Equations 3.24 and 3.25.

$$F_{nh} = (L)\sin(\lambda) + D\sin(\alpha) = 16.91\ lbf \tag{3.24}$$

$$F_{ph} = -(L)\cos(\lambda) + D\cos(\alpha) = 0\ lbf \tag{3.25}$$

These results show that for the mathematical model used to represent the boom, 16.91 lbf act normal to the boom and 0 lbf act perpendicular to the boom for 20 degrees angle of attack. These forces are the sum of dispersed loads acting along the full length of the boom.

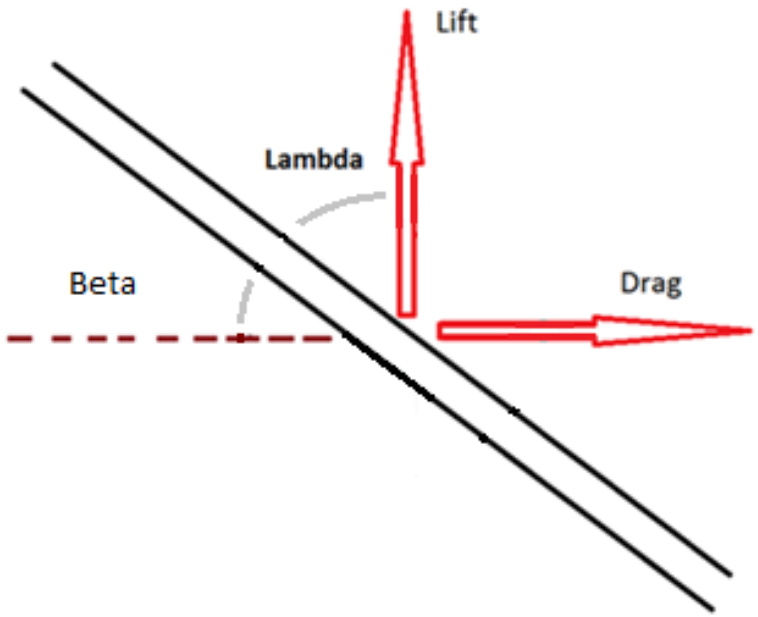

Figure 3.4: Free Body Diagram of Boom at an Angle of Sideslip

The total resultant forces acting normal and perpendicular to the boom are found using Equations 3.26 and 3.27 and the angle of the resultant force relative force from the lateral axis of the boom is found using Equation 28.

$$F_r = \sqrt{F_n^2 + F_{nh}^2} = 23.82\ lbf \tag{3.26}$$

$$F_p = \sum F_p = 1.52\ lbf \tag{3.27}$$

$$\Phi = tan^{-1}\frac{F_n}{F_{nh}} = 44.77\ deg \tag{3.28}$$

The results show that the mathematical model estimates a conservative total force of 23.82 lbf acting normal to the boom and 1.5 lbf acting perpendicularly to the normal force down the center line of the boom.

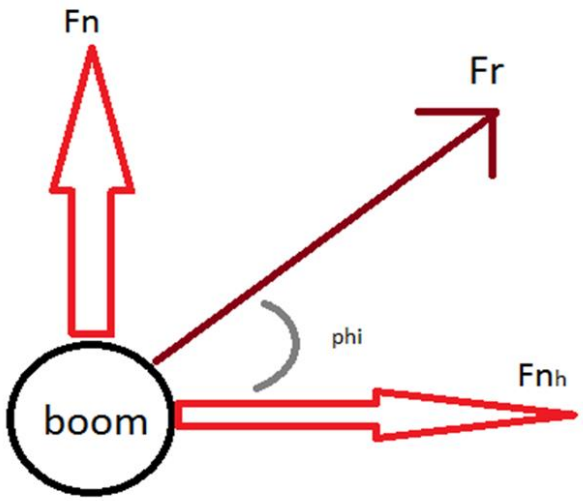

Figure 3.5: Free Body Diagram for Resultant Force Acting on the Boom

There are two ways to model the forces found from Equations 3.26 and 3.27. The first method is to model it as an evenly dispersed load acting along the center of the boom. The second method is to model the sum of the forces acting at the quarter chord as a conservative estimate for the center of pressure. Both models where used to find the reaction forces using the overdetermined beam solver and the first model had more conservative results and was used. To validate these assumptions, a flow simulation was performed using Solid Works Flow Simulation on a model of the boom. The boom was divided into 20 subsections and then solved for the drag forces acting at each subsection of the boom at 20 degrees angle of side slip and attack at V_{NE}. The resulting drag forces are set to act at the center of each sub-section and Equations 3.2 and 3.3 were used to find where the forces where centered at. The simulation showed the forces acted at a center of pressure ranging 39- 44" aft of the datum. This at 46.4-52% the length of the boom validating that the quarter chord assumption is a poor assumption for the structure of the boom.

Using a distributed load found using Equation 3.29, the reaction forces are found to be R_1=-80.46 lbs, R_2=85.31, and R_3=-28.67 using the online overdetermined system calculator [7].

$$\frac{Fr}{in} = {}^{F_r}/_{L_{total}} = {}^{23.82}/_{84.5} = .2835\ lbs/in \tag{3.29}$$

Using Equations 3.6 and 3.7 with the distributed load found in Equation 3.29, the shear and bending moment stress is solved for at any point, x, aft of the boom tip. The results are shown in Figure 3.6. It is clear that the highest stress point on the structure in at the front connector.

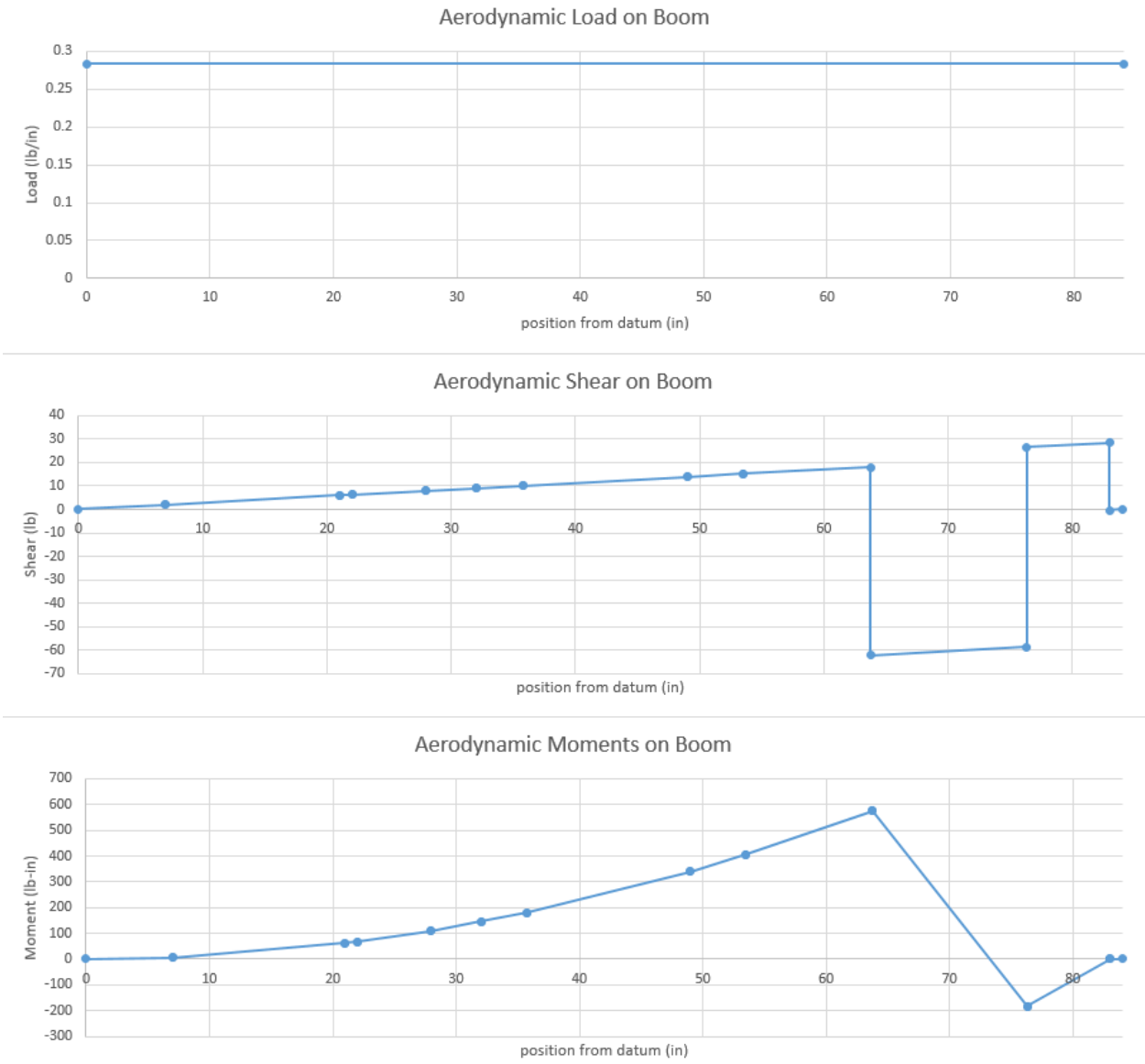

Figure 3.6: Loads, Shear and Bending Moments on Boom under Max Aerodynamic Loads

Applying the values found in Figure 3.6 to Equations 3.8-3.12 Give the maximum Von Mises Equivalent Stress and safety factor for each section of the boom shown in Table 3.5. While the forces caused by aerodynamic forces are considerably higher than those caused by high G loading the margin of safety is still high. Once again, this is expected since it is a relatively small structure that only has to support itself since the added drag of the vanes that weathercock into the relative wind is negligible.

Table 3.5: Stresses in Boom from Max Aerodynamic Stress

Section	Shear Stress, τ (psi)	Max Surface Stress, σ_{max} (psi)	Von Mises Stress, σ_e (psi)	Safety Factor, j
A	42.118	4535.777	4536.366	9.920
B	96.153	7569.477	7571.309	5.943
C	14.472	1233.436	1233.691	36.476
D	18.645	1722.336	1722.638	26.123
E	10.840	992.824	993.002	45.317
F	29.344	2833.710	2834.165	15.878
G	15.294	1525.652	1525.882	29.491
H	111.518	3279.008	3284.692	13.700
I	0.0005	0.361	0.361	124694.688

To find the deflection, y, of the boom the same process used for the G loading is applied with Equation 3.13 to get Equation 3.13d. This is in turn used to calculate the deflection at any point forward of the first connection, X_c. Equation 3.13 still uses a value of 10000000 psi for E and .067 for I.

$$y = (.0118)x_c^4 + (-3.013)x_c^3 + (288.17)x_c^2 \quad (3.13d)$$

This gives a conservative estimate for the max deflection of the boom tip to be .874 inches under the max aerodynamic stresses. Having already calculated the angle between the vertical and horizontal forces to be phi, Equation 3.16 can be modified to get Equation 3.16c and 3.16d to solve for the max errors in the alpha and beta vanes under max aerodynamic loads.

$$error\ in\ alpha\ angle = \arctan\left({y_{max} * \sin(\Phi)}/{63.76}\right) = .55^o \quad (3.16c)$$

$$error\ in\ beta\ angle = \arctan({y_{max} * \cos(\Phi)}/{63.76}) = .56^o \quad (3.16d)$$

These errors are small enough to not be an issue for the flight testing of the aircraft.

3.3 Bolt Shear

For the bolt shear, τ_b, calculations the bolt holding the highest calculated stress is evaluated. The bolt used is a 3/16 diameter aircraft steel (5Cr-Mo-V) with a bolt strength of 155000 psi [13]. The shear force of the bolt in the connector is found using Equation 3.30.

$$\tau_b = \frac{.5 * R_1}{2\pi D_b^2} = \frac{42.66}{2\pi\left(\frac{3}{16}\right)^2} = 193.1\ psi \quad (3.30)$$

The safety factor found using Equation 3.12 to be 912.64. The safety factor of the bolt is high and not a concern for the design and safety of the boom.

3.4 Bearing Stress

The bearing stress is calculated for the connector using the highest reaction stress previously found. The bearing strength of the material, AL 6061-T6, is 88000 psi [6] and is compared to the stress found in Equations 3.31 and 3.32 to get the safety factor of the bearing in Equation 3.33. In the equations D_b is the diameter of the bearing, t is the bearing thickness, and A_r is the reference area for he bearing stress shown in Figure 3.7.

$$A_r = D_b * t = \left(\frac{3}{16}\right).2 = .0375\ in^2 \tag{3.31}$$

$$\tau_{bearing} = {.5\ R_1}/{A_r} = {42.66}/{.0375} = 1137.48\ psi \tag{3.32}$$

$$j_{bearing} = {\sigma_{bearing\ ult}}/{\tau_{bearing}} = {118000}/{1137.48} = 77.36 \tag{3.33}$$

The safety factor is high and the bearing is not a critical point for the boom design.

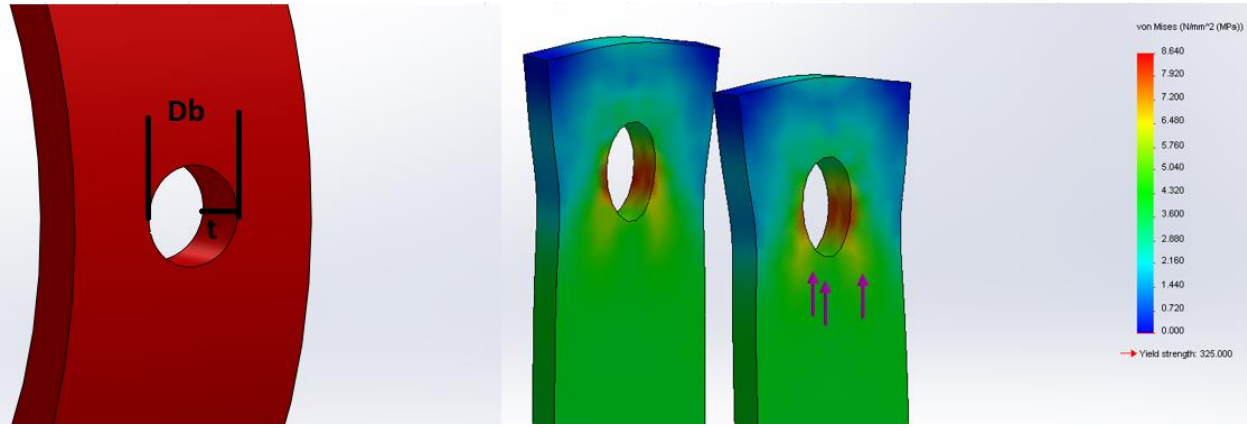

Figure 3.7: Bearing Diagram for Connector

3.5 L Bracket Bending

To model the L bracket only the bent aluminum piece is used for the mathematical stress calculations. The added thin plates under the bent piece and the aircraft spar and skin are ignored in order to get a conservative and simplified model. The bracket is modeled as a cantilever beam extended from the wing rib and supporting the reaction forces of the connections. The critical condition for the L bracket is for the highest reaction force of 85.31 lbf acting on connector 2. This puts a maximum stress right at the bend of the L bracket. This stress is a combination of the bending stress, Equations 3.34-3.37, and the shear stress, Equation 3.8. For the equations, t is the plate thickness, x_f is the distance from the bend to the point of the force, w is the plate width, and L is the length of the plate, shown in Figure 3.8.

$$M_b = R * x_f = 106.64\ lbf\ in \tag{3.34}$$

$$y = .5\ t = .0625\ in \tag{3.35}$$

$$I = w * t^3/12 = .000244\ in^2 \tag{3.36}$$

$$\sigma_b = {}^{M * y}/_{I} = 27300\ psi \tag{3.37}$$

The Von Mises Stress and safety factor is then found with Equation 3.11 and 3.12 with the ultimate strength of aluminum 2024-T2 being 45000 psi. This model of the L bracket has a max surface stress of 16379.71 psi, a shear stress of 682.49 psi, and a Von Mises Stress of 16507.18 psi. This gives the L bracket a safety factor of 2.73. This proves that the L bracket meets the strength requirements and should keep excessive forces from being applied to the wing skin or spar which could result in wing warping and a change in the aerodynamic qualities of the aircraft.

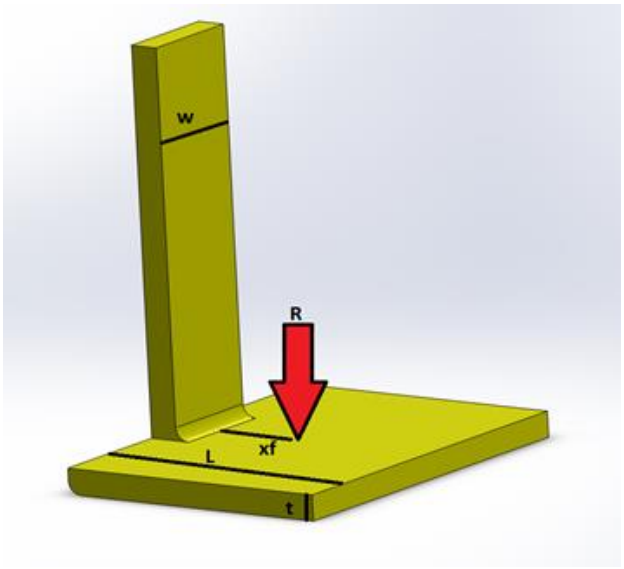

Figure 3.8: General L Bracket Stress Diagram

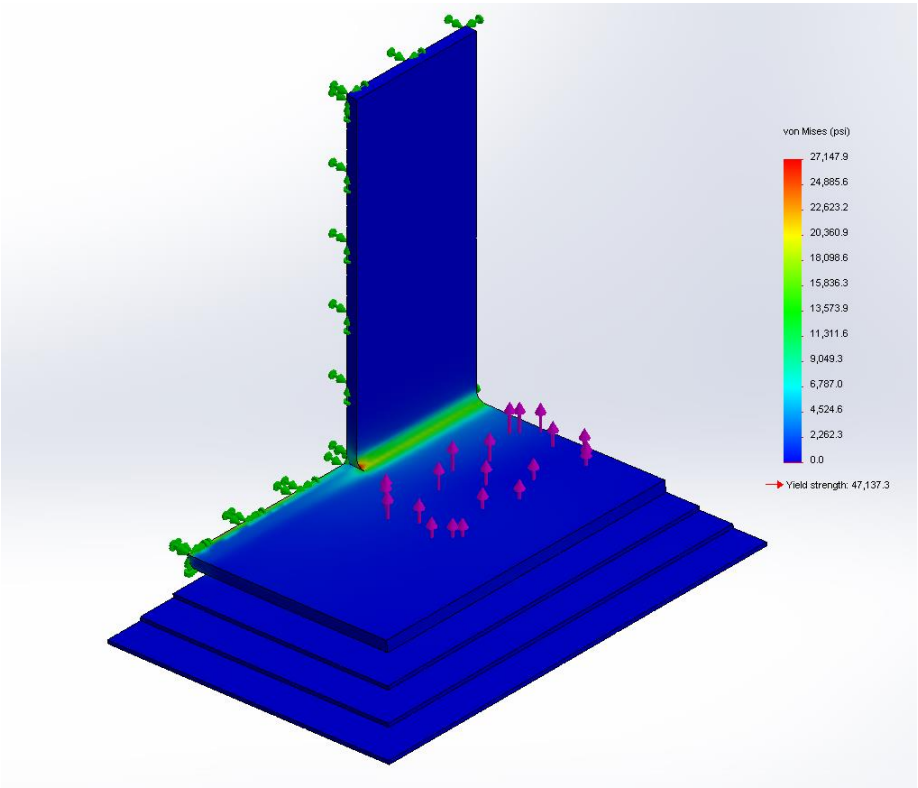

Figure 3.9: L Bracket Stress Simulation for Critical Center Bracket

3.6 Connector Stress

To model the connector, it is tested under the highest bending and shear forces present at the location of the connectors found in Section 3.1 and 3.2. The critical condition is thus the front connector under the max aerodynamic stresses, where the connectors is under an estimated 576.34 lbf bending moment and 62.38 lbs shear force. The area of the connector is provided by the Solid Works model to be .78 in^2 and the shear stress is calculated using Equation 3.8 to be 80.01 lbs. To find the max surface stress, the moment of inertia of the connector is treated like a half ring in Equation 3.38 and 3.39.

$$y = {}^{4(R_o^3 - R_i^3)}\Big/_{3\pi(R_o^2 - R_i^2)} = .54\ in \tag{3.38}$$

$$I = .1098\left(R_o^4 - R_i^4\right) - {}^{\left(.283R_o^2 * R_i^2 * (R_o - R_i)\right)}\Big/_{(R_o + R_i)} = .038\ in^4 \tag{3.39}$$

The max surface stress in then found using Equation 3.37 to be 8290.96 psi. This makes the Von Mises Stress to be 8292.12 psi and safety factor for the connector to be 5.43. This meets the minimum required safety factor of 1.5.

This model does not account for any forces present from the pinch on the connector when the widget is in place. These forces would act against the side loads from the G forces or aerodynamic drag from side slip and put a force on the tube structure. These forces are small and difficult to model and since the connectors and tube structure are modeled independently it is assumed that the added support of the connector would overpower the added pressure of the pinch and increase the safety factor.

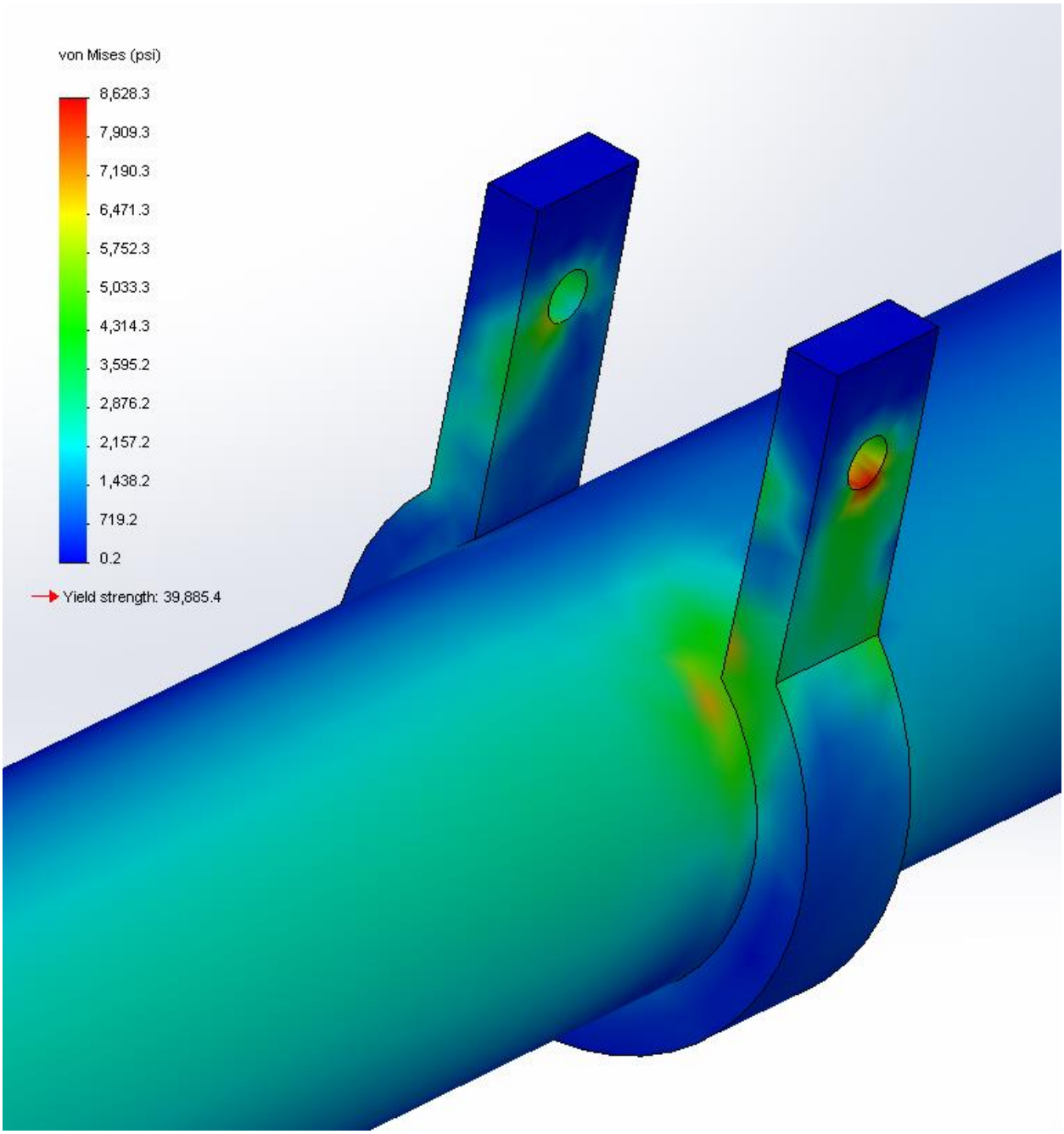

Figure 3.10: Connector Stress Test

3.7 Comparison of Final Results to Computer Simulations

In order to test the accuracy of the assumption made in my mathematical models and the accuracy of my hand calculations, all the models created in Solid Works are tested using a finite element analysis. The results for the mathematical models are compared to the finite element analysis to verify the results and are summarized in Table 3.6. The reason the max stresses are higher in the finite element analysis is that it takes into account the geometry of the connector creating a critical point. The model used for hand calculations treats the connections as evenly dispersing the load. As shown in Figures 3.11 through 3.14, the stress concentrates at the bend in the connectors giving the higher values for max stress. When the simulation was modified with fixed rings in place of the half ring connectors, the stress was solved to be slightly lower than the mathematical models, roughly 2400 psi. The deflection values calculated exceed the simulation by a good margin since the calculation model conservatively simplified the inertia values of the boom structure. Taking the most conservative values from both the calculated values and the finite element analysis still estimate the boom to have a large margin of safety under the tested conditions and little deflection to induce errors in the values recorded by the instrumentation. Both models also have the bend on the L bracket to be the weakest point on the structure.

Table 3.6: Stress Results of Calculations and Simulations

Model	Mathematical Model Calculations	Finite Element Analysis Simulation
G Load Max Stress	2896 psi	4879 psi
G Load Deflection	.550 in	.276 in
Max Angle Error	.47 degrees	.24 degrees
Aero Max Stress	3284 psi	5679 psi
Aero Deflection	.874 in	.51 in
Max Angle Error	.56 degrees	.33 degrees
L Bracket Stress	27376 psi	27148 psi
Connector Stress	8292 psi	8628 psi
Bearing Stress	1137 psi	1253 psi
Lowest Safety Factor	2.73	2.75

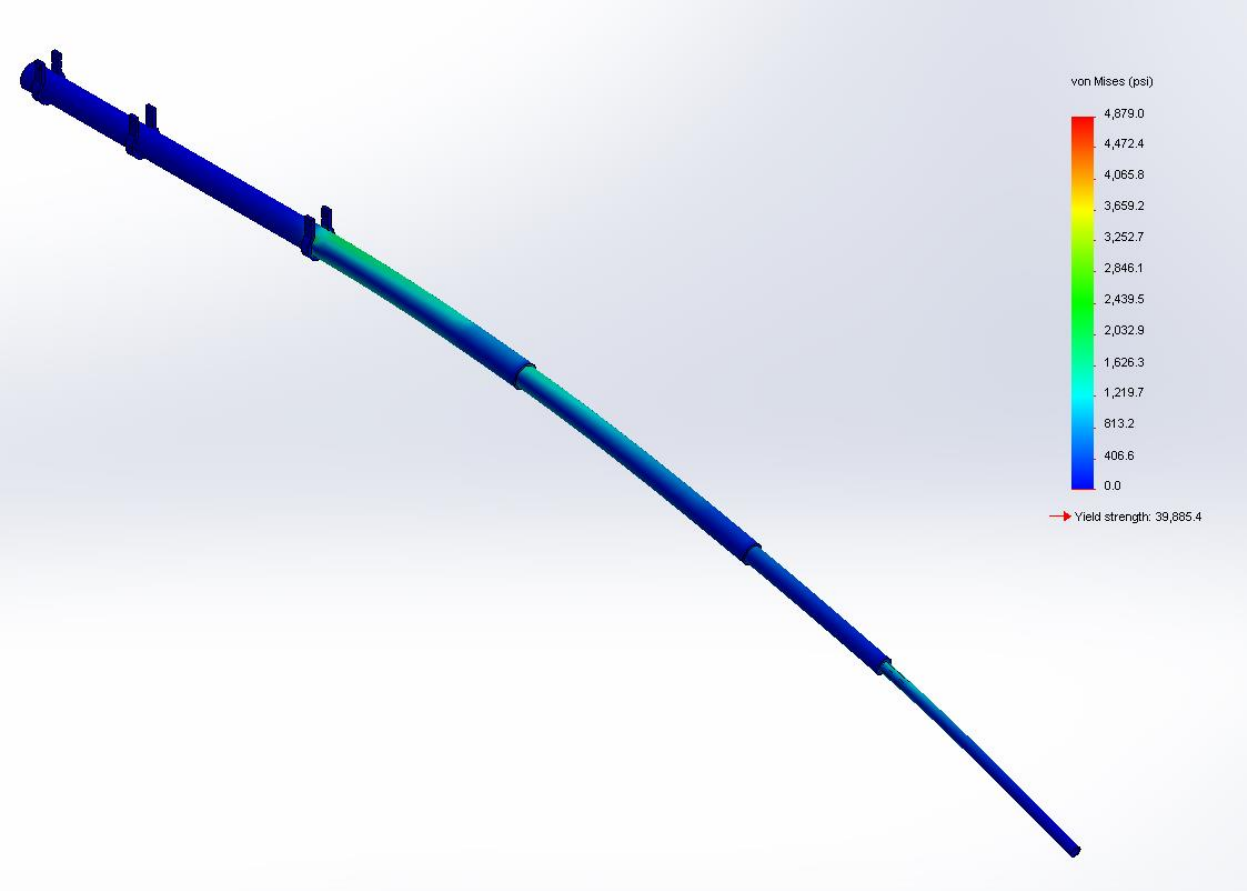

Figure 3.11: Stress from High G Loading

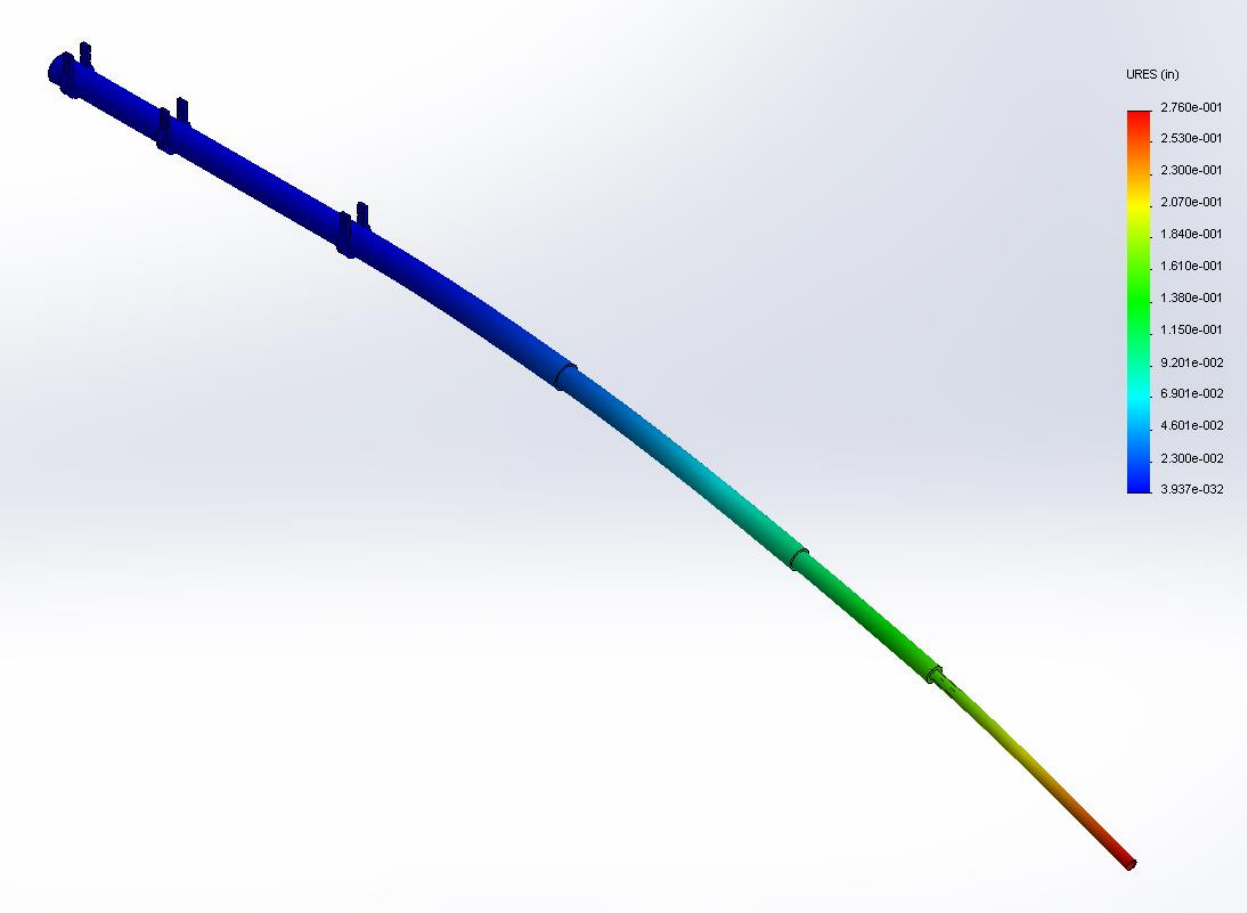

Figure 3.12: Displacement from High G Loading

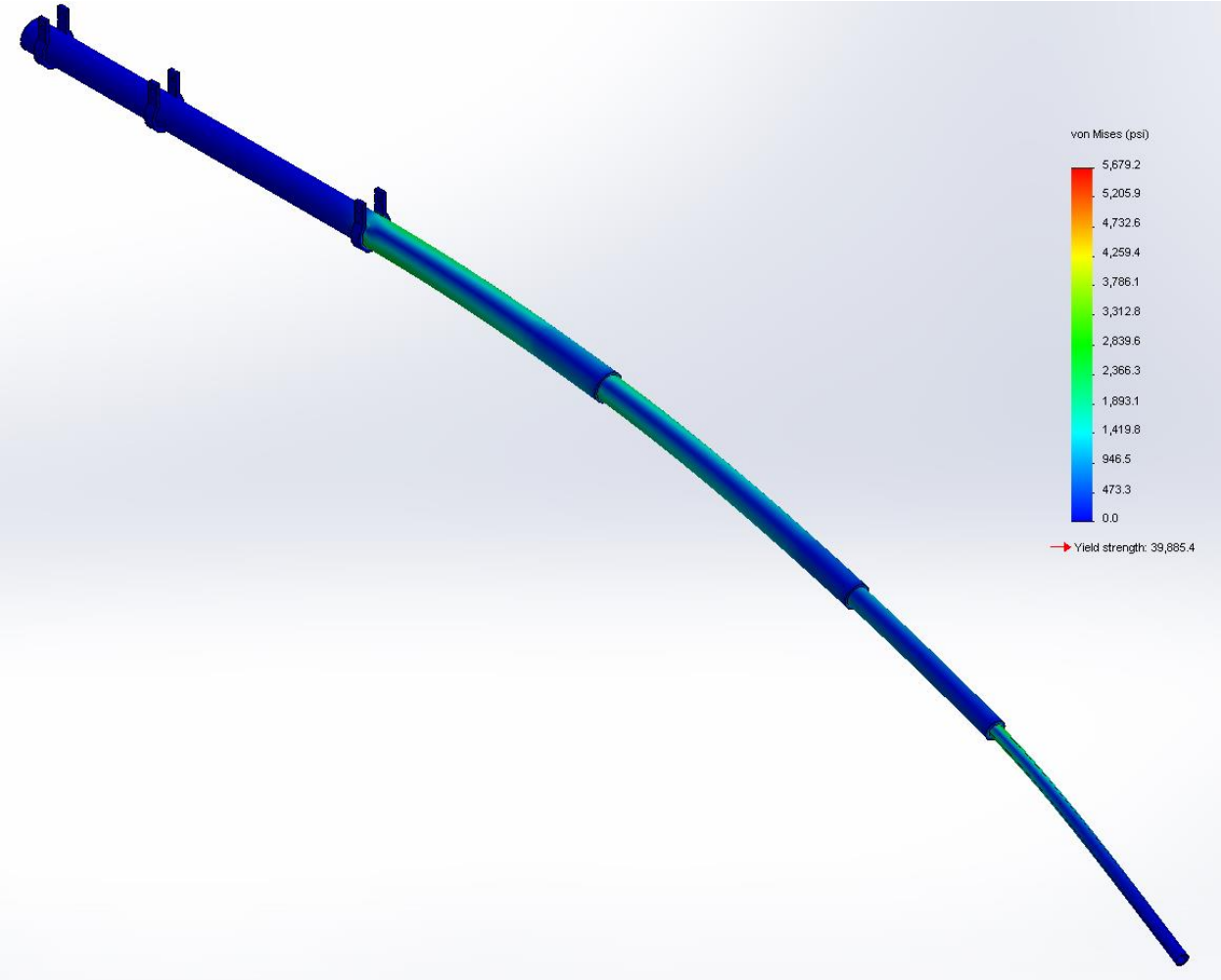

Figure 3.13: Stress from High Aerodynamic Stresses

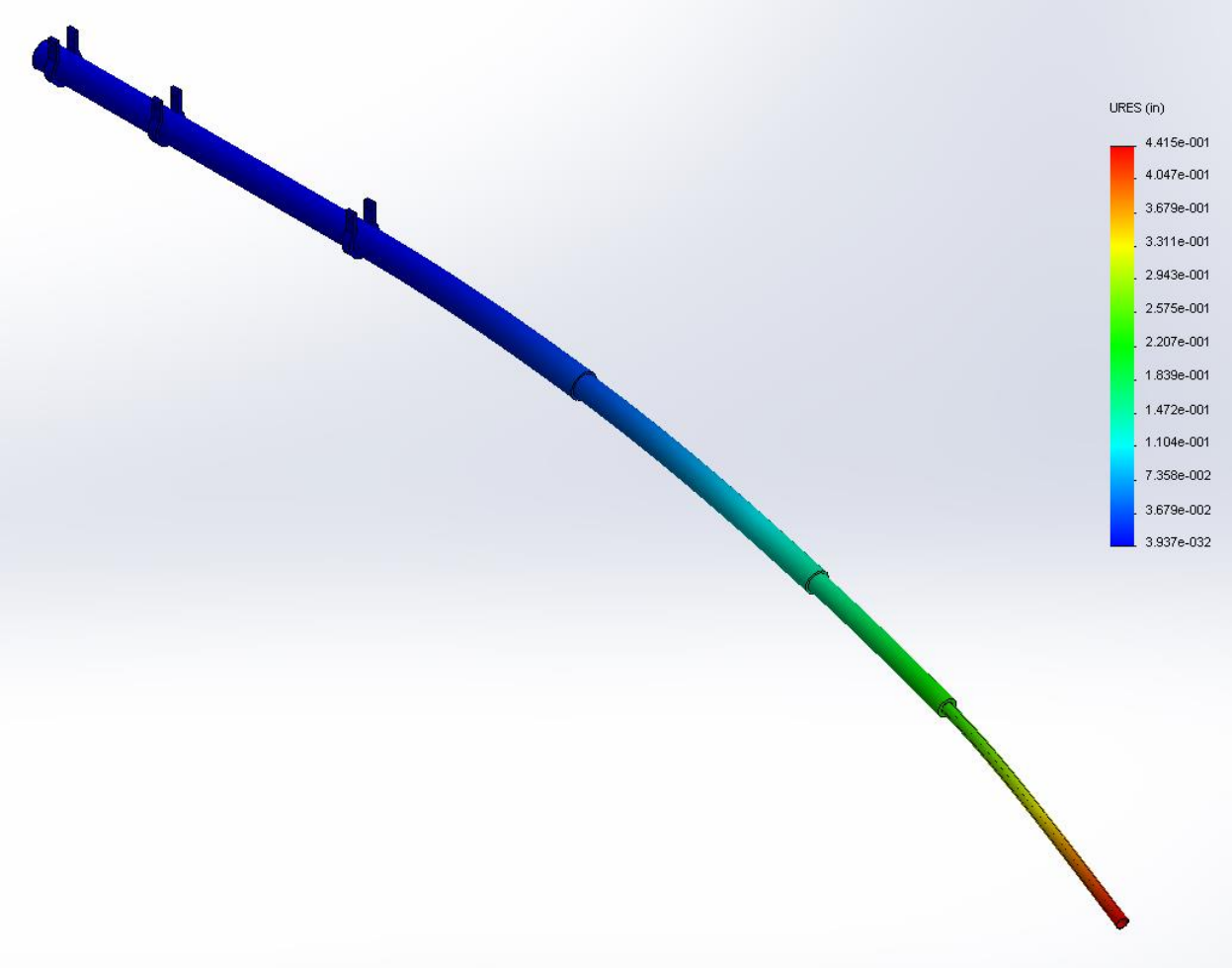

Figure 3.14: Displacement from High Aerodynamic Forces

A Solid Works Flow Simulation was performed on the boom structure to get values to compare to the calculated values of lift and drag. The flow simulation imitated an airflow of 344.67 ft/s with 20 angle of attack and side slip. The results of the simulation are compared to the calculated values in Table 3.7 with the x axis being parallel to the main structure, the y axis being vertically normal to the boom structure, and the Z axis pointing into the side slip. The Simulation estimates lower values of force than the calculations and does not show the same tend of the forces on the z axis being just slightly larger than the forces on the y axis. Since the simulation gives force values smaller than the critical conditions already tested it is not necessary to redo any of the calculations. The mathematical model used in Sections 3.1 and 3.2 assumed the force acting at the center of the boom and thus producing no torque forces. To check this assumption the flow study also solved for the total torque force acting on the full length of the boom structure. The force was found to be .0033 pound inches validating the assumption. The pressure distribution found by the simulation are shown in Figure 3.15.

Table 3.7: Drag Calculations vs Flow Simulation Results for Main Boom Structure

component	Calculated Estimate	Flow Simulation
Force along x axis	1.52 lbs	1.54 lbs
Force along y axis	16.78 lbs	13.14 lbs
Force along z axis	16.91 lbs	12.54 lbs
Torque along X axis	assumed insignificant	.000186 lb ft

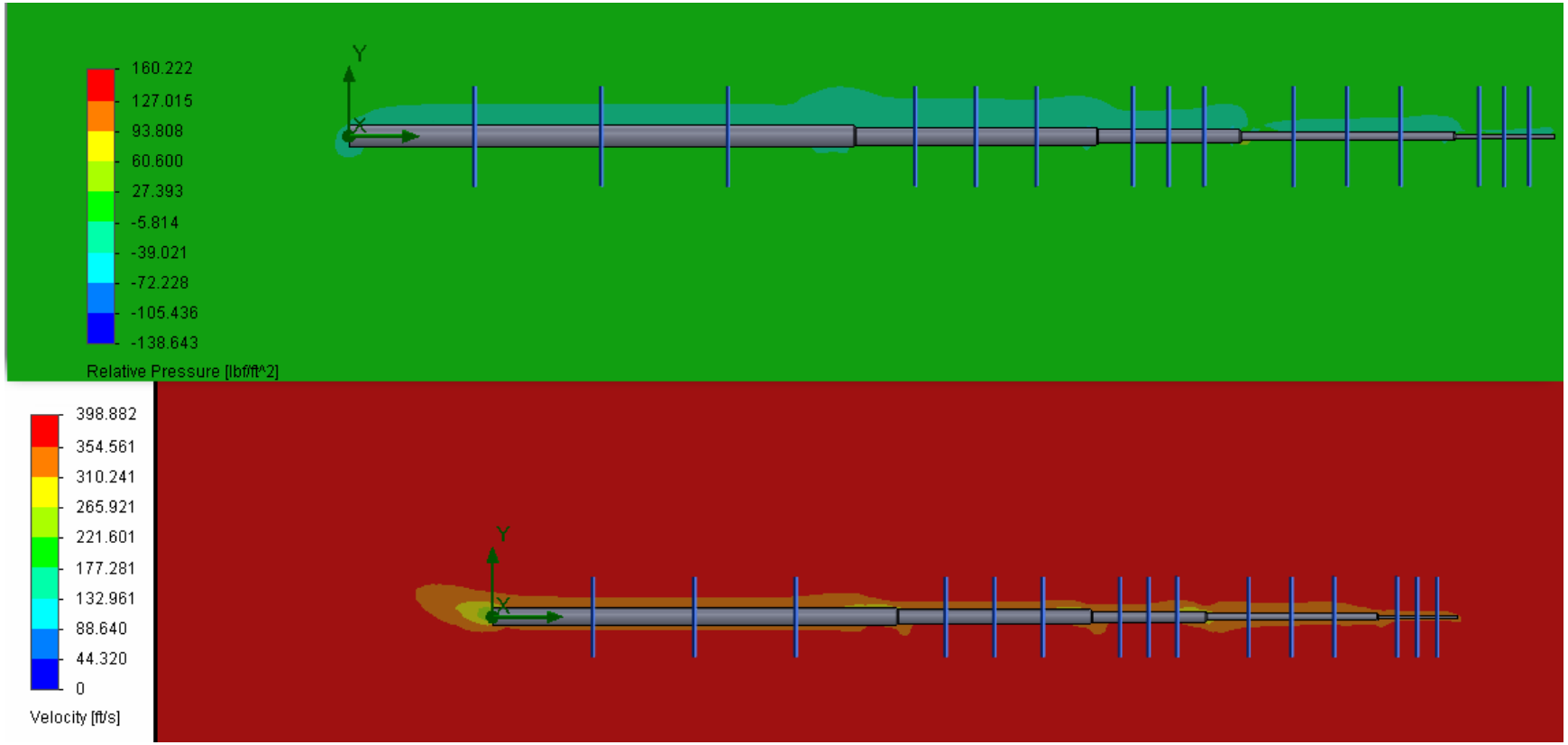

Figure 3.15: Solid Works Flow Simulation Cross Plots Results

3.8 Wing Torsion Calculation

It is necessary to ensure that forces acting on the boom do not create a strong enough moment about the torsional axis of the wing to effect the aerodynamic qualities of the aircraft. To find the exact torsional stresses around the wings elastics center would require extensive calculations beyond the scope of this thesis. In order to show that the effect of the boom is negligible, a conservative simplified model is used. The max coefficient of bending about the aerodynamic center of the wing is found using the NACA airfoil charts, Figure 3.17 to be Cm=-.4 [14]. The max coefficient is used in Equation 3.40 along with the max maneuvering airspeed, $V_{A,}$ of 125 knots for gross weight, sea level density, wing planform, and root chord length to find the max moment about the aerodynamic center, $M_{ac\ max}$ [8]. What exactly to use as the planform area, S, in Equation 3.40 has to be assumed for the situation. For these calculations the planform of the right wing is used under the assumption that the load would be dispersed over the entire wing. So the planform of the plane was divided by two to get the planform of just the right wing.

$$M_{ac\ max} = C_{m0}\frac{\rho}{2}v^2 S\bar{c} = -.4 * .00119 * 44511 * 75.4 * 4.10 = -6549.2\ lb\ ft \qquad (3.40)$$

The result from Equation 3.40 is compared to the moment caused by the aerodynamic forces of 125 knots at 20 degrees angle of attack and side slip acting on the boom, found using the process described in section 3.2, about the aerodynamic center of the wing found in Equation 3.41, shown in Figure 3.16.

$$M_{ac\ boom} = F_r(x_{ac\ boom} - x_{ac\ wing}) = 8.87(3.66 - 6.17) = -22.26\ lb\ ft \qquad (3.41)$$

It is clear that the wings contribution to the moment about the aerodynamic center overpowers the booms contribution. In order to relate the bending moments to values that are more applicable to the

pilot and flight test crew, Equation 3.40 can be rearranged to solve for the airspeed that the wing and boom produce a bending moment equal to the moment found in Equation 3.40.

$$v = \sqrt{(M_{ac\ wing} - M_{ac\ boom})/(C_{m0}\frac{\rho}{2}S\bar{c})} = 210.6\frac{ft}{s} = 124.8\ knots \qquad (3.40a)$$

So the bending moment normally caused at the V_A of 125 knots now occurs at 124.8 knots. Given the resolution of the equipment the pilots flies by, the change of .2 knots is insignificant and does not warrant changing the published V_A speed for the aircraft.

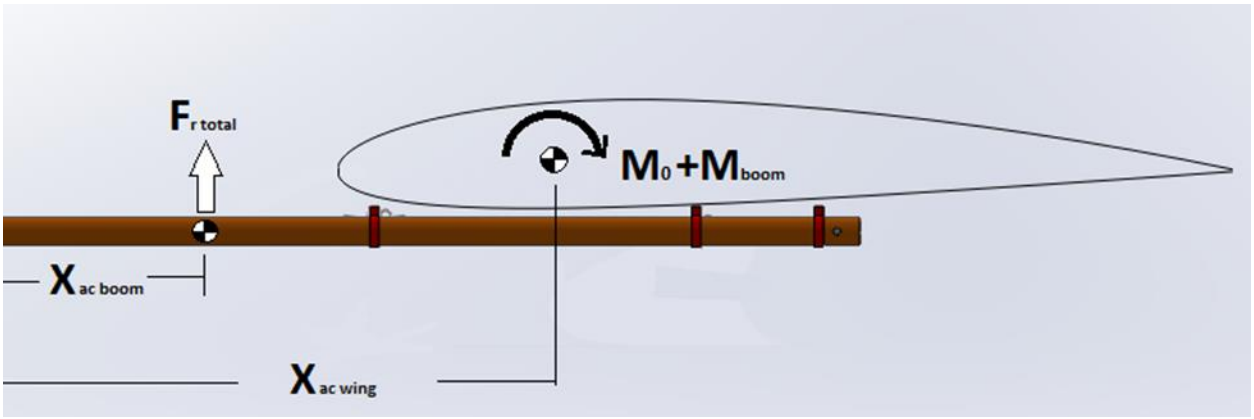

Figure 3.16: Booms Contribution to Moment about Aerodynamic Center of Wing

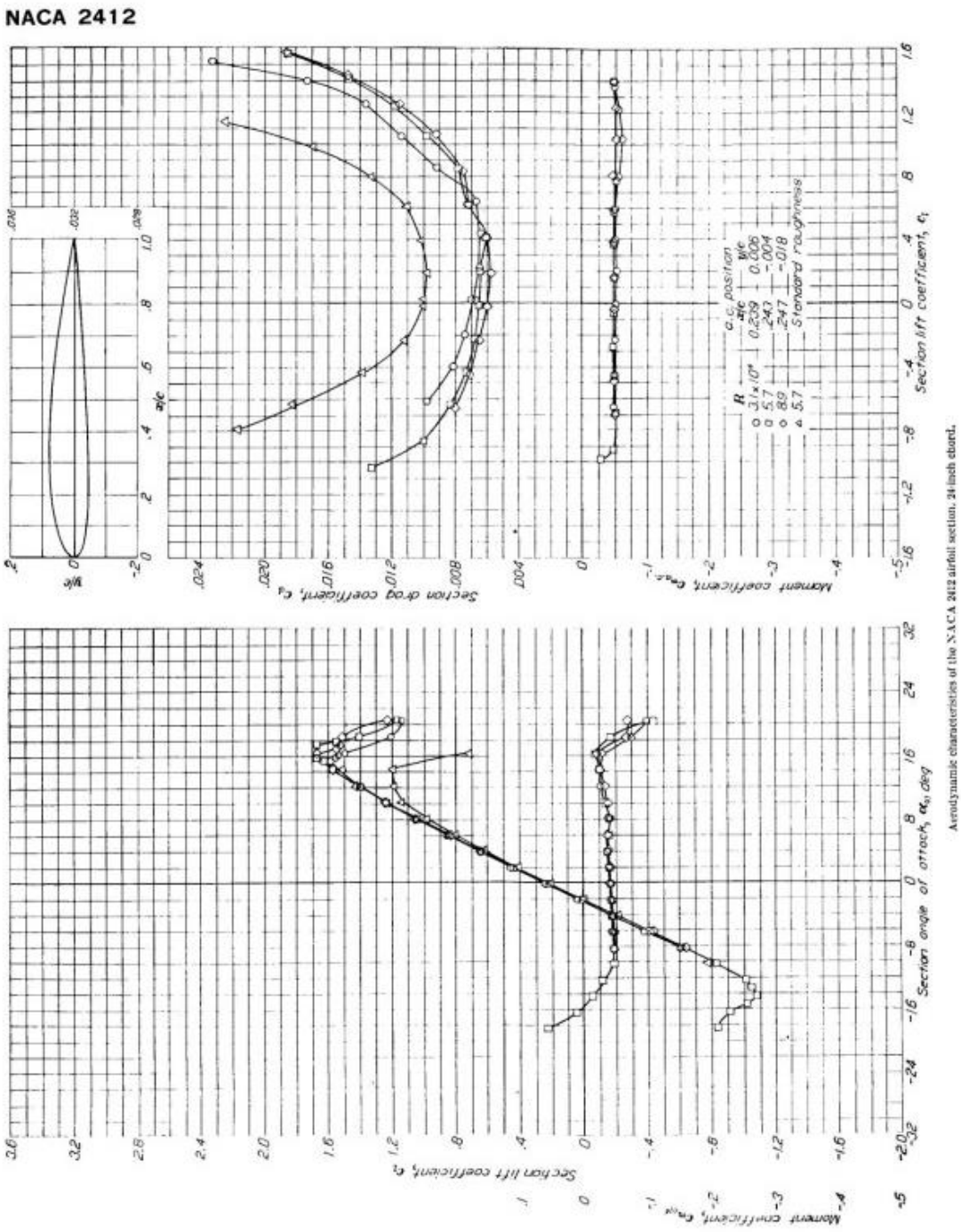

Figure 3.17: 2412 Airfoil Moment Coefficient Chart Provided by NACA

3.9 Wing Skin Torsion Shear

The booms added bending moment also adds to the wing skin's torsional shear. To insure that this added force does not create a safety hazard to the plane, the max bending stress allowed by the skin of the wing tip with a safety factor of 1.5. This is found by Equation 3.42-3.43 for the Bredt-Batho Shear Flow [15] and compared to the combined bending moments from Equation 3.40 and 3.41 for the bending moments of the wing plus the boom. The max skin stress for aluminum 2024 is 37000 psi, the skin thickness is .025 inches, and the cross-sectional area of the wing is found by solid works to be roughly 152.13 in^2.

$$q = t * 1.5\tau_{ult} = .025 * 37000/1.5 = 616.7\ lb/in \tag{3.42}$$

$$M_{t\ ult} = q * 2A = \ 616.7 * 2 * 152.13 = 187{,}627\ lb\ in = 15635.6\ lb\ ft \tag{3.43}$$

Equation 3.43 shows that the largest moment the wing skin can support is 15635.6 lb ft. This is larger than the combined moment of the boom and the wing of 6571.1 lb ft, with a safety factor of 2.4 times the ultimate strength.

3.10 Natural Frequency

To estimate the natural frequencies of the main boom structure, Solid Works Simulation was used to perform a frequency study on the structure. The computer model for the simulation consisted of the main structure and connectors only. The bearings in the connector are used as fixtures for the study. The study requires the structure to be one material so the entire boom is modeled as aluminum 6061-T6 despite the fact that the Space Age Control Mini Boom is an aluminum steel alloy. The results of the study are shown in Table 3.8. The engine operates in a range of roughly 1000 RPM to 2500 RPM so the frequencies are a concern when safety testing the boom. The engine mounts and aircraft structure

dampen the vibrations of the engine to a point that makes it unlikely they will stimulate the boom structures natural frequencies.

Table 3.8: Natural Frequencies of Main Boom Structure

Mode Number	Frequency
1	16.831 Hz (1010 RPM)
2	17.134 Hz (1028 RPM)
3	41.299 Hz (2478 RPM)
4	41.979 Hz (2519 RPM)
5	131.47 Hz (7888 RPM)

CHAPTER 4: TESTING AND CALIBRATIONS

4.1 Calibration of Pitot Static System

The pitot static system on the boom tip must be calibrated for use with the data acquisition system. To calibrate the static port to obtain altitude data, the static port is covered with a vacuum. The vacuum decreases the pressure to values that represent a range of pressure altitudes from standard atmosphere tables. At each pressure correlating to a pressure altitude the reading from the transducer attached to the static pressure line is recorded. The values input should cover the range of altitude the aircraft is expected to fly, 0 to 12,500 feet for the Cessna 210. The recorded values are plotted against the pressure altitudes generated by the vacuum to generate a trendline and equation. The equation generated in Excel is stored in the DAS files so values from the static port can be translated into altitude values.

The pitot static system is also calibrated to provide airspeed data. To accomplish this the pitot port is covered by a pressure chamber. The pressure in the chamber is increased to represent values of ram air in comparison to the static port. The values of pressure are related to a flow velocity using Equation 4.1, where P_t is the stagnation pressure being read by the ram air port, P_s is the static pressure from the static port, ρ is the air density, and *u* is the flow velocity. This is rearranged to get Equation 4.1a to solve for flow velocity.

$$P_t = P_s + ({}^{\rho u^2}/_{2}) \tag{4.1}$$

$$u = \sqrt{2(p_t - p_s)/\rho} \tag{4.1a}$$

Using Equation 4.1a the values for P_t, controlled by the pressure chamber over the pitot tube, and P_s, controlled by the vacuum chamber over the static tube, can be manipulated to represent values for

velocity, *u*. The desired values are plotted against the data from the transducers to get an equation that will translate the raw data into an airspeed value for the flight crew to monitor and record during testing.

At the University of Tennessee Space Institute the calibrations are accomplished by using a Barfield Digital Pitot Static Test Set. This equipment provides a digital user interface that simplifies and streamline the pitot static calibration by automatically adjusting the pressure to match airspeeds and altitudes as requested.

4.2 Calibration of Alpha and Beta Vanes

The alpha and beta vanes both need to be calibrated in order for the potentiometer readings to be translated into angle of attack and side slip for the DAS. To calibrate the vanes a mounted protractor is attached to the boom. The vanes are then manually adjusted to marked angles on the protractor and the values are matched to readings from the potentiometer. The readings and marked deflections are used to develop an equation for the DAS to translate the raw readings into useful angle information for the flight test crew. It is important to note that according to how the vanes are mounted the angle for zero deflection of the vanes may not correlate to zero angle of attack or side slip.

For this boom on the wing tip of the Cessna T210J Centurion the incidence angle of the wing is a concern. The wing has an incidence angle of +1.5 degrees at the root and -1.5 at the wing tip where the boom is installed [16]. This is done in order to provide more desirable stall characteristics for the aircraft. This means that when the angle of attack vane reads 0 degrees deflection from the boom structure it correlates to an angle of attack for the wing of -1.5 degrees. All the alpha reads will have to be calibrated with this -1.5 degrees correction. The boom structure is installed parallel to the chord line of the wing so there is no correction for the angle of side slip readings on the beta vane.

4.3 Ground Stress Testing

In order to stress test the installed boom structure a weight is hung from the structure at a certain location that imitates the max loads calculated in Chapter 3 of this report. The critical situations tested are the max G loading and max aerodynamic force loading. The distributed loads are simplified into a point load of an equivalent total value that act at the location of the CG for the G loading and the CP for the aerodynamic forces, shown in Figure 4.1. The equivalent load for the G load is found to be 21 pounds acting 47.3 inches from the boom tip at an angle of 18.4 degrees from vertically downwards. The aerodynamic load is found to be 24 pounds acting 42 inches from the tip at an angle of 45 degrees from horizontal. Both conditions are tested since the forces act in opposite directions. The main concern for the testing is the forces at the connections and L brackets, because those are the areas Solid Works predicted the lowest safety factors. For safety concerns the weight will be attached to the boom and laid on a surface that can be lowered and raised. The surface will slowly be lower so that the weight is allowed to hang free and exert forces on the boom. In case of any signs of failure, the surface below the weight can be quickly raised to unload the boom structure. In order to load the boom to imitate the aerodynamic loads acting upward a pulley system will be implemented. A tension gauge is used to measure the force in the line of the pulley system to insure that correct force is applied to the boom.

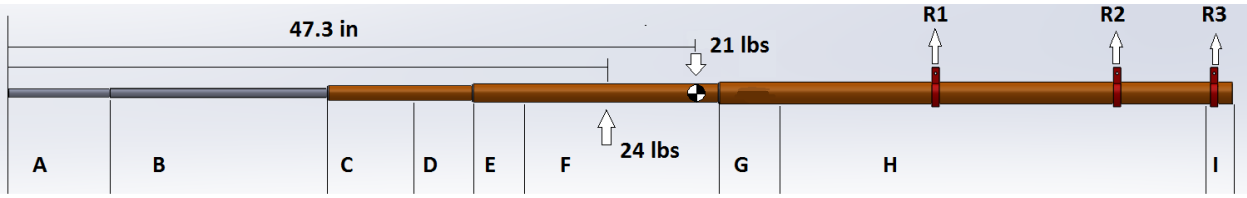

Figure 4.1: Equivalent Stress Test Loading

4.4 Ground Frequency Testing

Before a test flight is performed the boom is monitored during a ground run up to ensure that the boom is not stimulated by a natural frequency caused by the engine. This is achieved by running up the aircraft on the ground and slowly adjusting the power setting to achieve a full range of rpm setting for the aircraft. While this is done the boom is monitored from outside the aircraft to see if the boom begins to fluctuate dangerously during any part of the run-up procedure. If any of the engine settings do achieve a natural frequency in the boom structure, the engine should be shut down immediately to avoid damage to the aircraft. The boom would then have to be adjusted to change to natural frequency or to provide dampening to the boom.

4.5 Flight Testing

After the air data boom has passed all the ground testing the flight test can be performed. The importance of the flight test is to fly the pattern several times to insure that the boom does not affect the flying characteristics of the aircraft to any significant degree. The placement of the boom on the wing tip limits its' influence on the airflow over the wing. The boom will generate drag causing a right yawing force, but this force should be overpowered by the left turning force of the three blade propeller. It is also possible that the drag of the boom could create rolling tendency by either disrupting the air flow over the right wing tip causing a loss of lift, and a right roll, or by the boom generating lift on the right wing tip causing a left roll. In either case the effect of the boom is predicted to be negligibly small and easily corrected with trim. Overall, the boom should have an insignificant effect to the flying characteristics of the aircraft.

Before the boom is used for the flight testing, an air data system calibration test should be performed to correct any position error in the system. The easiest way to do this is a 4 leg GPS method

calibration. The details of this kind of flight test are not covered in the scope of this paper. It is also advised to perform a series of stall test in order to see if the stall speed of the aircraft is changed by the boom. Given the size and position of the air data boom, the stall speed should not be changed to any significant degree but this can not be confirmed without testing.

The frequency the flight data is recorded at during flight test is dependent of the setup of the equipment. The potentiometers used to measure the vanes reading for angle of sideslip and angle of attack are an analog system. Any analog reading is recorded at the frequency the DAS is set to at the time of the flight test. The rate the altitude and airspeed are recorded at are dependent of the type of potentiometer the pressure lines are attached to. If the potentiometer is analog it will record at whatever rate the DAS is set to, but if it is digital it will be limited by the device. At the time of writing a potentiometer is not installed on the aircraft, but a Honeywell Precision Pressure Transducer is the recommended equipment for flight test applications. The transducer should be designed for the pressure range expected from flight testing of a static pressure of roughly 8 psi for static pressure at high altitudes up to roughly 17 psi for stagnant pressure at standard sea level and V_{NE}.

CHAPTER 5: CONCLUSIONS

This boom was designed with the goals of being a cord length ahead of the wing tip to gather good data, to be relatively unbending while under forces to gather good data, and to have a structure that can withstand all the stresses caused in flight. The design is successful in all these concerns and when properly calibrated provides valuable flight test data. The extensive calculations and computer simulated testing of the boom structure show that the boom is rigid and structurally strong in comparison to the forces it will experience. The excessive safety factor of the structure can be defended by the need of the boom to be stiff while experience high winds and G forces from maneuvering. The data for angle of attack and sideslip will now be available while flying the Cessna T210J. The booms pitot static system will provide more accurate data for airspeed and altitude, than the aircraft commercial system.

The steps described in this thesis could be used to design similar booms structures for use on other small aircraft. The main change I would make to the design process if I was to create another boom, would be to approach the design from the parts available. The original design first envisioned had to be greatly altered and recalculated due to difficulty finding and machining the parts necessary. I would also prefer to gather frequency information from the aircraft before the design process. Equipment could be placed on the wing at the same location the boom would be attached to record the frequency range experience while running the engine through its full operating range. Early design could be tested in simulations to ensure that the boom's natural frequency do not fall in this range. Due to maintenance being performed on the aircraft and time limitations, I was not able to do frequency testing on the aircraft prior to the design process.

LIST OF REFERENCES

[1] *Turbo Centurion Cessna model T2101L: Pilot's operating handbook.* (1976). Wichita, Kan.: Cessna Aircraft.

[2] Spaceagecontrol.com: Main Data Sheet - 100400 Mini Air Data Boom. (n.d.). Retrieved January 29, 2015.

[3] FAA. (2014). *FAR/AIM 2015 Federal Aviation Regulation 23.337.* New York: Skyhorse Publishing.

[4] Airfoil Tools. (n.d.). NACA 2412 (naca2412-il). Retrieved January 30, 2015, from http://airfoiltools.com/airfoil/details?airfoil=naca2412-il

[5] Peters, B., Hendricx, W., & Debille, J. (2009). Modern Solutions for Ground Vibration Testing of Large Aircraft. *Sound & Vibration/ January 2009*. Retrieved January 29, 2015, from http://www.sandv.com/downloads/0901peet.pdf

[6] MatWeb. (n.d.). ASM Material Data Sheet. Retrieved January 29, 2015, from http://asm.matweb.com

[7] Terekhov, D. (2008, January 1). Beam Analysis (calculation) online. Retrieved January 29, 2015.

[8] Raymer, D. (1999). Aircraft design: A conceptual approach ([3rd ed.). Reston, VA: American Institute of Aeronautics and Astronautics.

[9] Engineering Edge (n.d.). Section Modulus. Retrieved January 30, 2015, from http://www.engineersedge.com/material_science/section_modulus_12893.htm

[10] von Mises, R. (1913). *Mechanik der festen Körper im plastisch deformablen Zustand.* Göttin. Nachr. Math. Phys., vol. 1, pp. 582–592.

[11] Bucciarelli, L. (2002, January 1). Chapter 8: Deflection due to bending. Retrieved January 29, 2015, from http://web.mit.edu/emech/dontindex-build/full-text/emechbk_8.pdf

[12] Hoerner, S. (1965). *Fluid-dynamic drag: Practical information on aerodynamic drag and hydrodynamic resistance*. Alburqueque, N.M.: Db Hoerner Fluid Dynamics.

[13] SAE International. (n.d.). SAE Standards. Retrieved January 30, 2015.

[14] Abbott, I., Von Doenhoff, A., & Stivers, L. (1945). Report No. 824 Summary of Airfoil Data. *National Advisory Committee for Aeronautics*.

[15] Megson, T. (2007). *Aircraft structures for engineering students* (4th ed.). Oxford: Butterworth-Heinemann.

[16] *Centurion series, 1970 thru 1976 service manual* (Changed 1975. ed.). (1975). Wichita, Kan.: Cessna Aircraft.

VITA

Kristopher Oegema was born in Knoxville, TN, to the parents Gamble and Gerald Oegema. He is second of three children with an older sister Brittany and a younger brother Cory. He attend Bearden High School in Knoxville then went on the Middle Tennessee State University for and undergraduate degree in Aviation Technology with two minors in Mathematics and Engineering Technology. He then decided to further his education with a Masters of Science in the Flight Test Engineering program at the University of Tennessee Space Institute in Tullahoma.